Electronic Supplementary Information

Exquisite Sensitivity of The Ligand Field to Solvation and Donor Polarisability in Coordinatively Saturated Lanthanide Complexes

Kevin Mason[a], Alice C. Harnden[a], Connor W. Patrick[a], Adeline W. J. Poh[a], Andrei S. Batsanov[a], Elizaveta A. Suturina[b], Michele Vonci[c], Eric J. L. McInnes,[c] Nicholas F. Chilton[c] and David Parker * [a]

General Procedures

All solvents were laboratory grade and anhydrous solvents were stored under argon in a septum-capped bottle. Water was purified by the 'PuriteSTILLplus' system, with a conductivity of $\leq$ 0.04 μS cm^{-1}. Commercially available reagents were used as received. Air sensitive reactions were carries out using Schlenk link techniques under argon. Thin layer chromatography was performed on silica plates (Merck Art 5554) or neutral aluminium plates (Merck Art 5550) and visualised under UV irradiation at 254 nm, or by staining with iodine. Preparative column chromatography was performed using silica gel (Fluorochem Silica Gel 60, 230-400 mesh) or neutral alumina (Merck Aluminium Oxide 90, activity II-III, 70-230 mesh), with the latter pre-soaked in ethyl acetate overnight before use.

NMR Spectroscopy

^{1}H and ^{13}C NMR spectra were recorded in commercially available deuterated solvents on a Varian Mercury-200 (^{1}H at 199.975, ^{13}C at 50.289, ^{19}F 188.179), Varian Mercury-400 (^{1}H at 399.960, ^{13}C at 100.572, ^{19}F 376.338), Bruker Avance-400 (^{1}H at 400.052, ^{13}C at 100.603, ^{19}F 376.423), Varian Inova-500 (^{1}H at 499.722, ^{13}C at 125.671, ^{19}F 470.253), Appleby VNMRS-600 (^{1}H at 599.832, ^{13}C at 150.828, ^{19}F 564.385), or Varian VNMRA-700 (^{1}H at 699.731, ^{13}C at 175.948, ^{19}F 658.405) spectrometer. All chemical shifts are quoted in ppm and all coupling

constants are reported in Hz. Paramagnetically shifted proton assignments were aided by relaxation measurements; the recorded free induction decays were processed using backward linear prediction, optimal exponential weighting, zero-filling, Fourier transform, phasing and baseline correction (by polynomial fitting or Whittaker smoothing). The signals were integrated by Lorentzian line fitting. ^{1}H longitudinal relaxation times were measured at 295 K using the inversion-recovery technique, on spectrometers operating at fields of 4.7 and 9.4 T. Each relaxation time measurement was repeated three times to reduce experimental error. The number of transients used in the measurements was determined by the signal-to-noise ratio of the sample. The incremented delay time was set to show full inversion and full recovery to equilibrium of the signal to minimise the experimental error. Fitting errors were determined by calculating the standard deviation of a set of relaxation times.

Optical Methods

All solution state optical analyses were carried out in quartz cuvettes with a path length of 1 cm. Measurements were recorded at 295 K. UV/Vis absorbance spectra were measured on either an ATI Unicam UV/Vis spectrometer (Model UV2) using Vision software (version 3.33) or an Agilent Cary 5000 UV-Vis-NIR spectrometer using WinUV software (version 4.1). Emission spectra were recorded using either an ISA Jobin-Yvon Spex Fluorolog-3 luminescence spectrometer using DataMax software (version 2.2.10) or a HORIBA Jobin-Yvon Fluorolog-3 luminescence spectrometer equipped with an iHR320 module, which selects either a HORIBA FL-1073 (Hamamatsu R928P) photomultiplier tube, a Hamamatsu thermoelectric cooled H10330B-75 NIR-photomultiplier tube or a HORIBA Synapse BIDD CCD for detection of emitted light, using FluorEssence software (based on Origin® software).

Mass Spectrometry

Electrospray mass spectra were obtained on a TQD mass spectrometer equipped with an Acquity UPLC system, an electrospray ion source and an Acquity photodiode array detector (Waters Ltd., UK). Accurate masses were recorded on an LCT Premier XE mass spectrometer or a QToF Premier Mass spectrometer,

both equipped with an Acquity UPLC, a lock-mass electrospray ion source and an Acquity photodiode array detector (Waters Ltd., UK). Methanol or acetonitrile were used as the carrier solvents.

X-ray crystallography

X-ray single crystal data were collected on a Bruker 3-circle D8 Venture diffractometer with a Photon100 CMOS detector, using Mo-Kα radiation (λ = 0.71073 Å) from a IμS-microsource with focusing mirrors. The crystals were cooled to 120 K with a Cryostream (Oxford Cryosystems) open-flow N2 cryostat. The data were corrected for absorption by numerical integration based on crystal face-indexing (for [Yb.L^4] by semi-empirical method based on Laue equivalents and multiple scans) using SADABS program.[X1] Structure [Yb.L^5] was solved by direct methods using SHELXS program,[X2] [Yb.L^4] by charge-flipping method using SUPERFLIP program,[X3] and the rest by dual-space intrinsic phasing method using SHELXT program.[X4] All structures were refined using SHELXL software[X5] on OLEX2 platform.[X6] Absolute structure of [Yb.L^5] and polarity of [Yb.L^1] were determined by Flack-Parsons method.[X7] Selected crystal data and experimental details are listed in Table S1, full crystallographic information (including structure factors) in CIF format has been deposited with Cambridge Crystallographic Data Centre and is available as 1849021-1849027 and 1850294, raw diffractometer data is available from the authors, citing the local depository number.

All complexes have essentially the same *molecular* structures, apart from the effects of the different ionic radii of Yb^{3+} and Eu^{3+} ions. All crystals were racemic except [YbL^5] which underwent spontaneous resolution and was studied as the Λ-(δδδ) enantiomer (for comparison, the same enantiomer was chosen as the reference molecule in the racemic structures). Concerning the *crystal* structures, [Yb.L^1]·$3H_2O$ is isomorphous with the previously reported Eu, Gd, Lu, Nd[X8] and Tb[X9] analogues, [Eu.L^3]·$6H_2O$ is isomorphous with [Yb.L^3]·$5H_2O$·MeOH, but [Eu.L^5] and [Yb.L^5] crystallise in different lattices, with different amounts of water.

References- X-ray crystallography

X1. L. Krause, R. Herbst-Irmer, G.M. Sheldrick and D. Stalke, *J. Appl. Crysallogr.*, 2015, **48**, 3-10.
X2. G.M. Sheldrick, *Acta Crystallogr.*, 2008, **A64**, 112-122.
X3. (a) L. Palatinus and G. Chapius, *J. Appl. Crysallogr.*, 2007, **40**, 786-790; (b) L. Palatinus and A. van der Lee, *J. Appl. Crysallogr.*, 2008, **41**, 975-984; (c) L. Palatinus, S. J. Prathapa and S. van Smaalen, *J. Appl. Crysallogr.*, 2012, **45**, 575-580.
X4. G.M. Sheldrick, *Acta Crystallogr.*, 2015, **A71**, 3-8.
X5. G.M. Sheldrick, *Acta Crystallogr.*, 2015, **C71**, 3-8.
X6. O.V. Dolomanov, L.J. Bourhis, R.J Gildea, J.A.K. Howard and H. Puschmann, *J. Appl. Crystallogr.*, 2009, **42**, 339-341.
X7. (a) S. Parsons and H.D. Flack, Acta Crystallogr. 2004, **A60**, s61; (b) S. Parsons, H.D. Flack and T. Wagner, *Acta Crystallogr.*, 2013, B69, 249-259.
X8. C. Gateau, M. Mazzanti, J. Pécaut, F.A. Dunand and L. Helm, *Dalton Trans.*, 2003, 2428-2433.
X9. G. Nocton, A. Nonat, C. Gateau and M. Mazzanti, *Helv. Chim. Acta*, 2009, **92**, 2257.

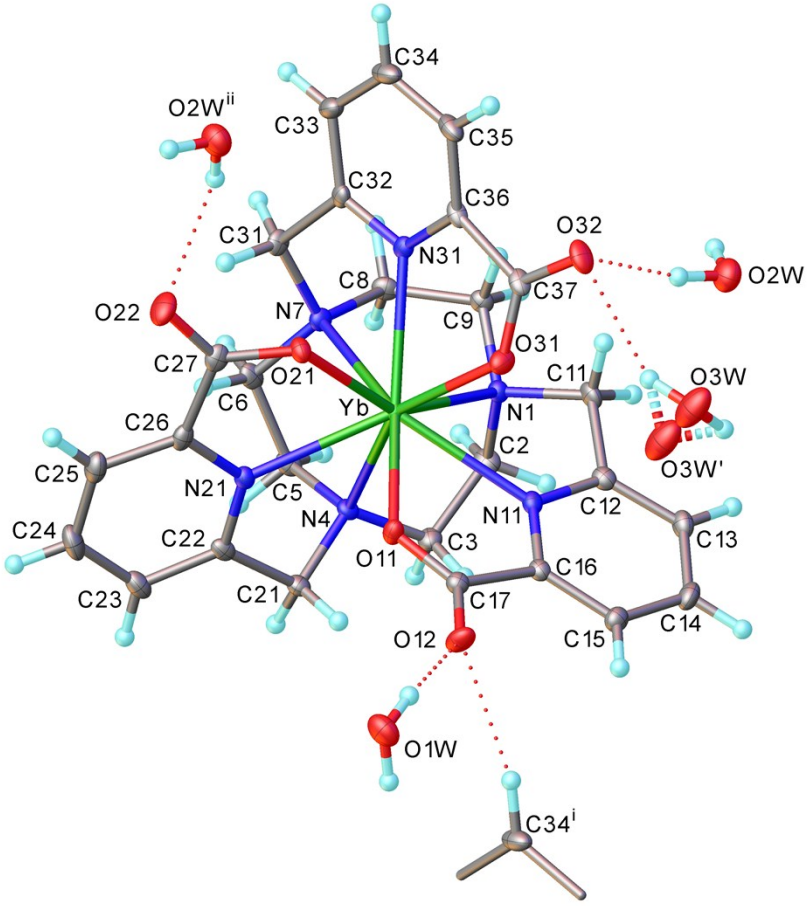

Figure S1. Molecular structure of [YbL^{1}]·3H$_2$O showing hydrogen bonds (see Table S2). Here and below, thermal ellipsoids are drawn at the 50% probability level. O(3W) is disordered between two positions with occupancies 0.8 and 0.2 (primed). Symmetry transformations: (i) ½+*x*, 1–*y*, ½+*z*, (ii) *x*, *y*–1, *z*.

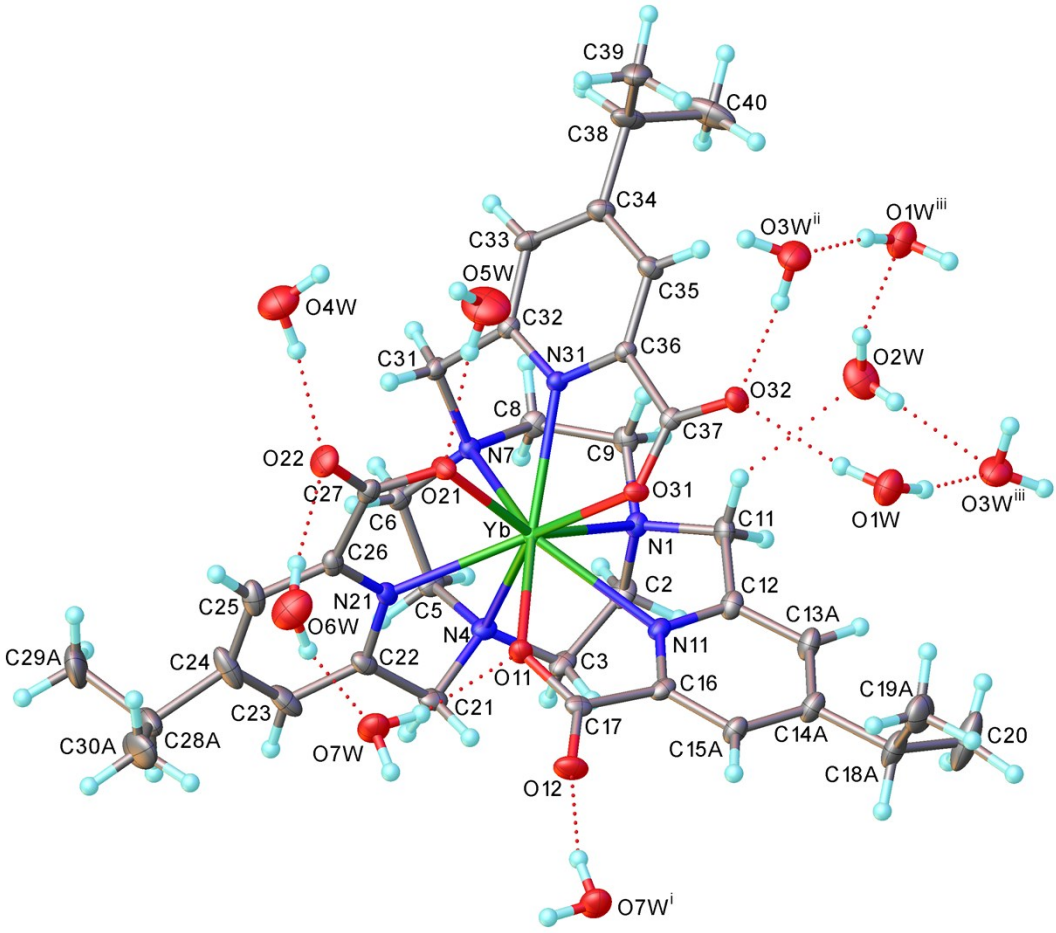

Figure S2. Molecular structure and hydrogen bonding of [Yb.L^2]·7H_2O. Disorder is not shown (see Fig. S3). Symmetry transformations: (i) –*x*, –1–*y*, –2–*z*, (ii) *x*+1, *y*, *z*, (iii) –*x*, –*y*, –1–*z*.

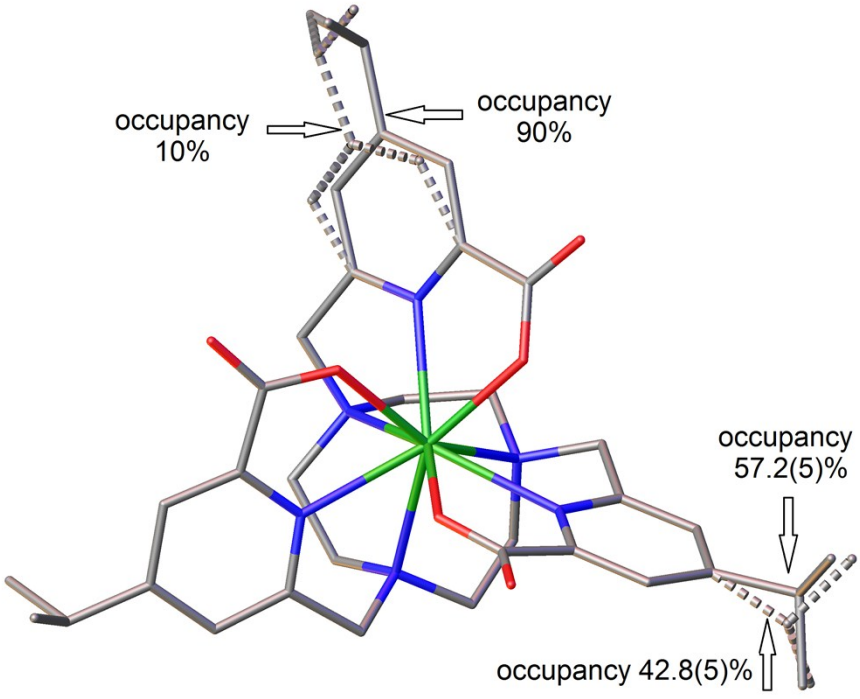

Figure S3. Disorder in the molecule of [YbL^2]. H atoms are omitted for clarity.

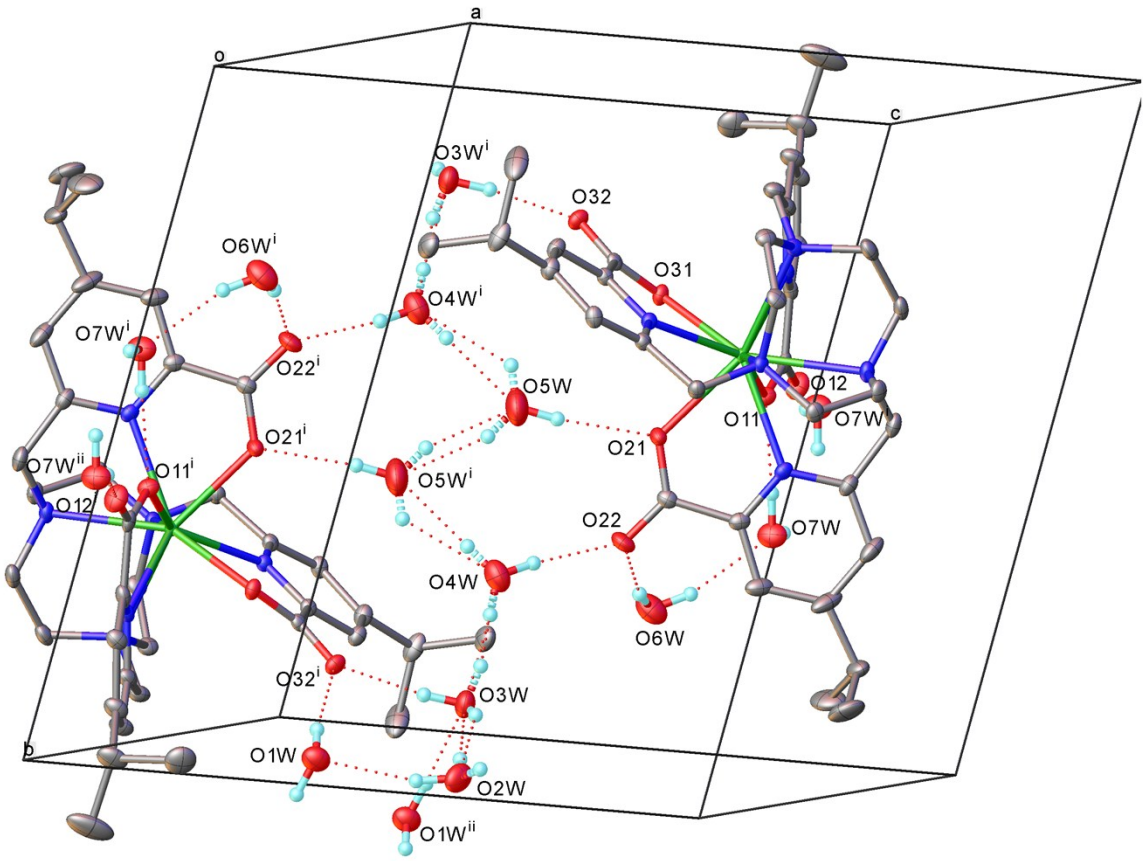

Figure S4. Crystal packing of $[YbL^2]\cdot 7H_2O$. Symmetry transformations: (i) 1–*x*, 1– *y*, 1–*z*, (ii) –*x*, 2–*y*, 1–*z*. H atoms, except those of water, are omitted. The pairs O(2W) and O(3W), O(3W) and O(4W), O(4W) and O(5W), O(5W) and its inversion equivalent, are each linked by two hydrogen bonds of opposite polarity with equal (50%) probability.

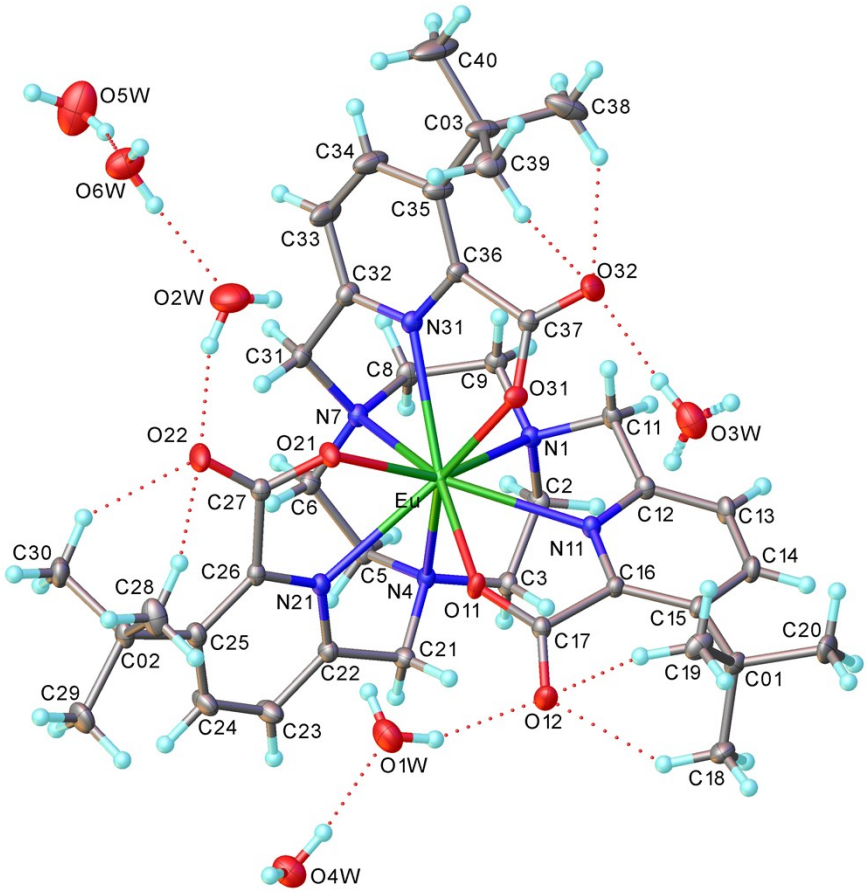

(a)

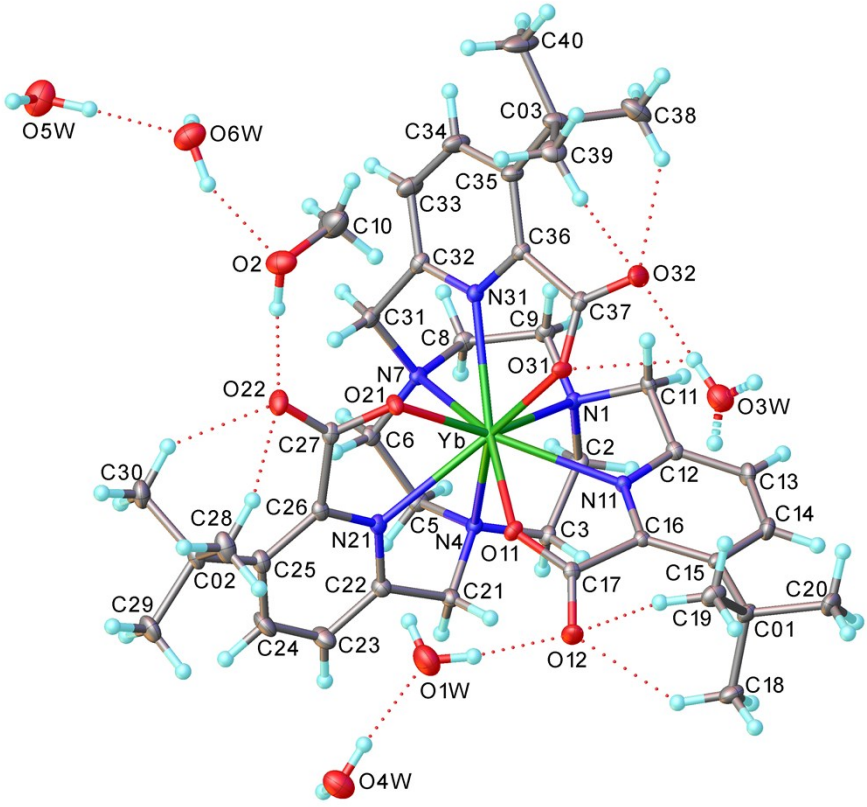

(b)

Figure S5. Molecular structure and hydrogen bonding in [Eu.L^3]·6H_2O (a) and [Yb.L^3]·5H_2O·MeOH (b).

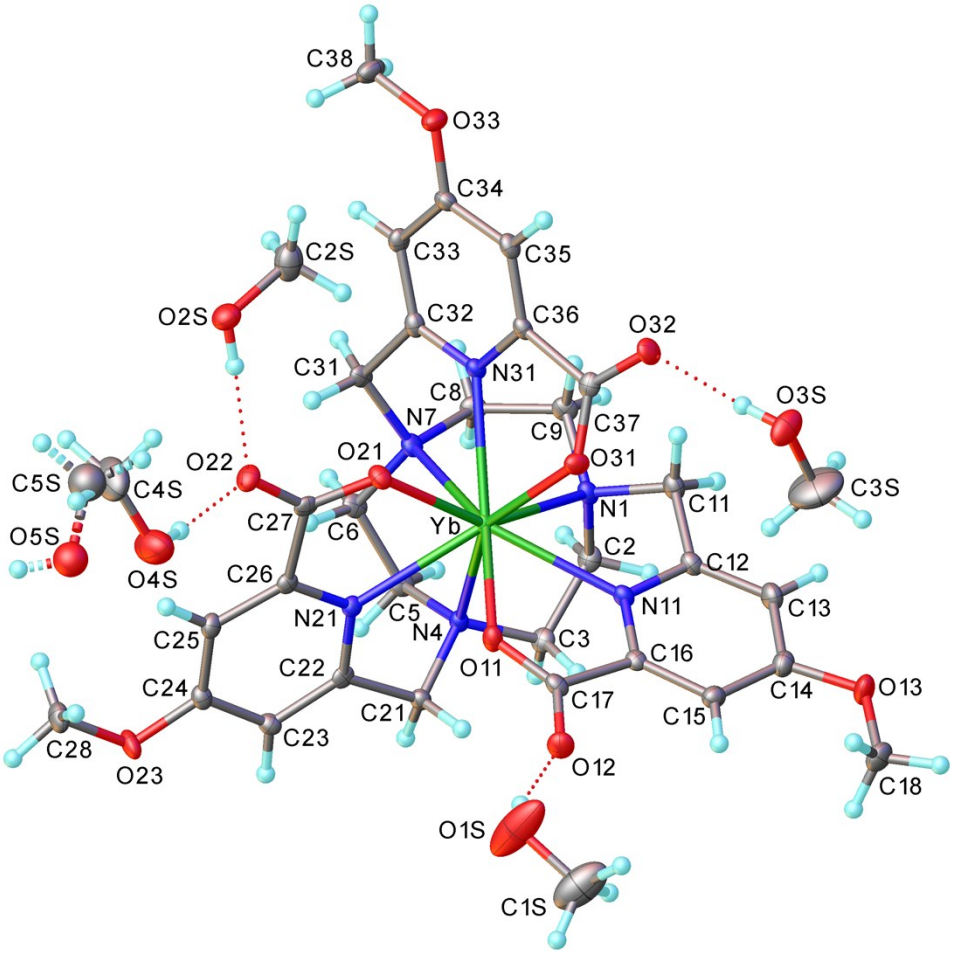

Figure S6. Molecular structure and hydrogen bonding of [Yb.L^4]·4MeOH. One methanol molecule is disordered between two positions with occupancies 85% (solid) and 15% (dashed).

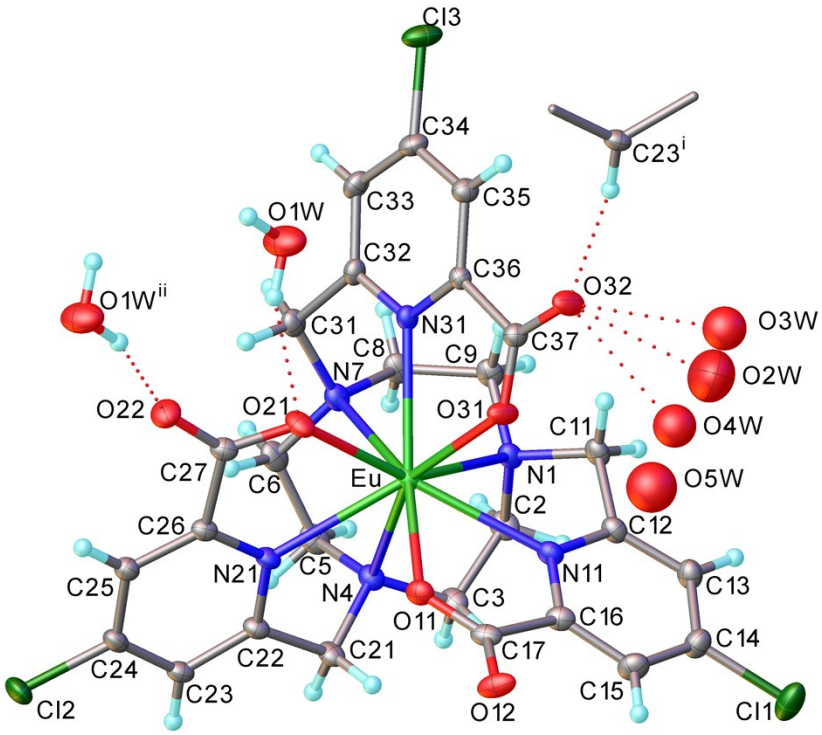

Figure S7. Molecular structure and hydrogen bonding of [Eu.L[5]]·2.5H_2O, showing alternative positions of the disordered water. Symmetry transformations: (i) –*x*, –1–*y*, –1–*z*, (ii) *x*, *y* – 1, *z*.

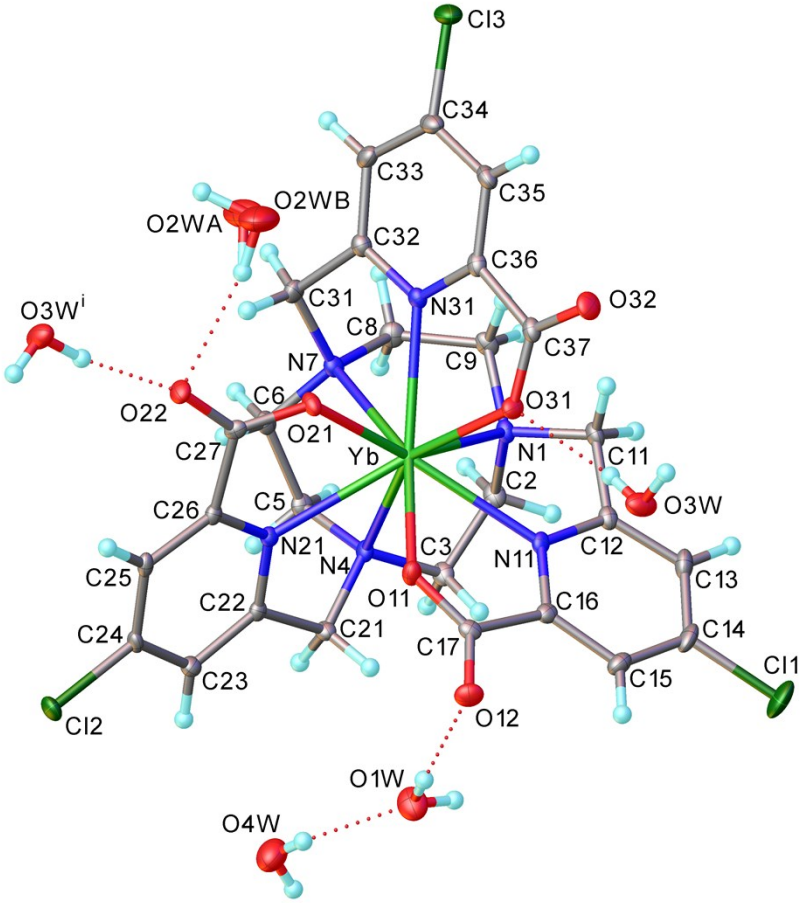

Figure S8. Molecular structure and hydrogen bonding of [Yb.L[5]]·4H_2O. Symmetry transformation: (i) 1–*x*, y+½, ½–z.

Table S1. Crystal data and experimental details

Compound	$[YbL^1]\cdot 3H_2O$	$[YbL^2]\cdot 7H_2O$	$[EuL^3]\cdot 6H_2O$	$[YbL^3]\cdot 5H_2O\cdot MeOH$		$[YbL^4]\cdot 4MeOH$	$[EuL^5]\cdot 2.5H_2O$	$[YbL^5]\cdot 4H_2O$
Depository no.	18srv253	18srv061	18srv142	18srv194	18srv194a	18srv138	18srv120	18srv176
CCDC no.	1850294	1849021	1849022	1849023	1849024	1849025	1849026	1849027
Formula	$C_{27}H_{33}N_6O_9Yb$	$C_{36}H_{59}N_6O_{13}Yb$	$C_{39}H_{63}EuN_6O_{12}$	$C_{40}H_{65}N_6O_{12}Yb$		$C_{34}H_{49}N_6O_{13}Yb$	$C_{27}H_{29}Cl_3EuN_6O_{8.5}$	$C_{27}H_{32}Cl_3N_6O_{10}Yb$
Formula weight	758.63	956.93	959.91	995.02		922.83	831.87	879.97
$D_{calc.}$/ g cm^{-3}	1.854	1.583	1.456	1.504	1.510	1.659	1.852	1.876
μ/mm^{-1}	3.509	2.399	1.497	2.195	2.203	2.604	2.435	3.326
Size/mm^3	0.30×0.05×0.02	0.61×0.20×0.07	0.30×0.14×0.14	0.39×0.14×0.12		0.19×0.08×0.04	0.28×0.17×0.07	0.57×0.14×0.06
T/K	120	120	120	160	120	120	120	120
Crystal System	monoclinic	triclinic	triclinic	triclinic	triclinic	triclinic	triclinic	orthorhombic
Space Group	Pn (no. 7)	$P\bar{1}$ (no. 2)	$P\bar{1}$ (no. 2)	$P\bar{1}$ (no. 2)	$P\bar{1}$ (no. 2)	$P\bar{1}$ (no. 2)	$P\bar{1}$ (no. 2)	$P2_12_12_1$ (no. 19)
a/Å	7.9466(3)	8.0215(3)	7.5667(5)	7.6574(3)	7.6432(3)	7.8898(3)	8.0370(8)	7.8822(4)
b/Å	11.7823(5)	14.8835(6)	13.2216(9)	13.1494(5)	13.1291(6)	14.8884(6)	11.9227(12)	17.4071(8)
c/Å	14.7072(6)	17.6485(7)	22.7804(15)	22.7470(9)	22.7386(9)	15.9436(7)	17.541(2)	22.7074(11)
α/°	90	106.9911(15)	87.639(3)	86.530(2)	86.5326(17)	95.4509(16)	109.078(3)	90
β/°	99.3301(14)	90.0945(17)	87.556(3)	86.957(2)	86.9081(17)	93.4986(15)	90.559(4)	90
γ/°	90	94.4990(17)	74.190(3)	74.094(2)	74.1063(17)	96.4015(15)	108.769(3)	90
V/Å^3	1358.81(10)	2008.17(14)	2189.8(3)	2197.08(15)	2188.87(16)	1847.88(13)	1491.5(3)	3115.6(3)
Z	2	2	2	2	2	2	2	4
$2\Theta_{max}$/°	67.5	71.4	71.4	71.6	66.3	60	67.7	68
Reflections total	36972	55290	55878	60349	43241	40729	39992	84745
unique	10726	16744	18135	18394	16639	10767	11866	12648
with $I > 2(I)$	9393	14376	16219	15744	14193	8888	10179	11660
R_{int}	0.042	0.041	0.031	0.034	0.034	0.047	0.037	0.044
Parameters refined	391	566	550	554	553	513	425	462
$\Delta\rho_{max,\,min}$/eÅ^{-3}	0.89, -0.93	1.10, -0.90	2.28, -4.29	1.97, -2.09	2.06, -1.97	0.84, -0.73	1.34, -1.06	0.66, -0.68
Goodness of fit	0.984	1.024	1.236	1.060	1.038	0.989	1.041	1.020
R_1, wR_2 (all data)	0.038, 0.046	0.037, 0.055	0.049, 0.099	0.044, 0.064	0.044, 0.067	0.044, 0.056	0.039, 0.063	0.027, 0.042
R_1, wR_2 [$I > 2(I)$]	0.027, 0.044	0.026, 0.054	0.041, 0.097	0.032, 0.062	0.032, 0.065	0.030, 0.054	0.028, 0.061	0.021, 0.041
Flack parameter x	-0.017(4)							-0.015(2)

Table S2. Hydrogen bonds D–H…A in complexes [Ln.L^{1-5}]·Solv [a]

Complex	A	C-O(A)	D	D…A /Å	H…A [b] /Å	D-H-A [b] /°
[YbL^1]·3H_2O	O(12)	1.234(4)	Water	2.783(4)	1.95	165.4
			CH(aryl)	3.179(5)	2.27	161.2
	O(22)	1.229(5)	Water	2.836(4)	2.14	138.3
	O(32)	1.237(5)	water	2.857(4)	2.03	163.6
			Water [e]	3.052(5)	2.27	153.8
[YbL^2]·7H_2O	O(11)	1.274(2)	water	3.004(2)	2.18	164.2
	O(12)	1.233(2)	water	2.791(2)	1.97	160.7
	O(21)	1.272(2)	water	2.941(2)	2.10	173.2
	O(22)	1.242(2)	water	2.820(2)	1.98	172.8
			water	3.040(2)	2.20	169.4
	O(32)	1.245(2)	Water	2.829(2)	1.99	170.6
			water	2.736(2)	1.89	173.8
[EuL^3]·6H_2O	O(12)	1.233(3)	water	2.763(3)	1.98	152.9
			Methyl [c]	3.049(4)	2.25	138.4
			Methyl [c]	3.094(4)	2.31	136.6
	O(22)	1.234(3)	Water	2.764(4)	2.00	149.6
			Methyl [c]	3.010(4)	2.19	139.8
			Methyl [c]	3.098(4)	2.31	136.4
	O(32)	1.234(3)	water	2.857(4)	2.01	171.9
			Methyl [c]	3.033(4)	2.22	139.3
			Methyl [c]	3.091(4)	2.30	137.4
[YbL^3]·5H_2O·MeOH	O(12)	1.235(2)	water	2.746(2)	1.91	165.7
			Methyl [c]	3.068(3)	2.27	137.5
			Methyl [c]	3.068(3)	2.27	137.8
	O(22)	1.232(2)	methanol	2.727(2)	1.82	172.5
			Methyl [c]	3.002(3)	2.19	139.4
			Methyl [c]	3.110(3)	2.34	135.1
	O(32)	1.232(3)	water	2.806(2)	1.97	168.1
			Methyl [c]	3.025(3)	2.22	139.0

			Methyl [c]	3.064(3)	2.27	137.4
$[YbL^4]\cdot 4MeOH$	O(12)	1.232(3)	methanol	2.772(3)	1.95	164.0
	O(22)	1.244(3)	methanol	2.782(2)	1.94	176.4
			methanol	2.832(3)	2.00	171.4
	O(32)	1.231(3)	methanol	2.770(3)	1.93	173.9
$[EuL^5]\cdot 2.5H_2O$	O(12)	1.228(2)	-----			
	O(21)	1.269(2)	Water	3.058(2)	2.30	147.8
	O(22)	1.235(2)	Water	2.893(2)	2.07	163.6
	O(32)	1.230(2)	water [e,f]	2.904(5)	?	?
			CH(aryl)	3.156(2)	2.22	169.3
$[YbL^5]\cdot 4H_2O$	O(12)	1.241(3)	Water	2.785(3)	1.94	170.7
			Water	2.848(3)	2.01	166.8
	O(22)	1.238(3)	Water	2.835(3)	1.99	172.4
			Water [d]	2.963(16)	2.18	153.7
			Water [d]	2.978(18)	2.18	157.1
	O(32)	1.223(3)	---			
	O(31)	1.285(3)	water	2.863(3)	2.02	169.6

[a] O(n2) – carbonyl oxygen, O(n1) – Ln-bound carboxylate oxygen; [b] for O–H bonds normalised to 0.85 Å, C(sp^3)–H to 0.98 Å, C(sp^2)–H to 0.95 Å; [c] intramolecular contacts; [d] alternative positions of the disordered water (50% occupancies); [e] major position of the disordered water; [f] H atoms not located

General labelling scheme of [Ln.L$^{1\text{-}5}$] protons

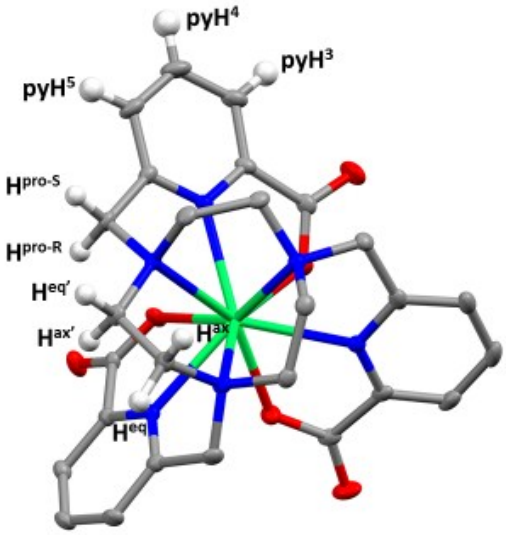

Figure S9 Labelling scheme used throughout the NMR analysis. Ring axial and equatorial protons are labelled 'ax' and 'eq' respectively; pyridyl protons are labeled 'py'. Nitrogen donor atoms appear as blue and carboxylate oxygens as red.

HPLC analysis

Reverse phase HPLC was performed at 295 K using either a Shimadzu system comprising a Degassing Unit (DGU-20A5R), a Prominence Preparative Liquid Chromatography pump (LC-20AP), a Prominence UV-Vis Detector (SPD-20A) and Communications Bus Module (CBM-20A) or an Interchim Puriflash 4250 equipped with an iQuat HPLC pump, a 200-400 nm UV-DAD detector and a fraction collector. For preparative HPLC either an XBridge C18 OBD column (19 × 100 mm, 5 μm) with a flow rate of 17 mL/min or an ACE C18-PFP column (10 × 50 mm, 5 μm) with a flow rate of 4.5 mL/min was used. Fraction collection was performed manually. A solvent system of H_2O/MeCN (Methods A, B and C) or H_2O/MeOH (Method D) was used with gradient elution as follows:

Method A

Step	Time / min	% H_2O	% MeCN
0	0	90	10
1	3	90	10

2	13	0	100
3	18	0	100
4	20	90	10

Method B

Step	Time / min	% H_2O	% MeCN
0	0	90	10
1	3	90	10
2	13	0	100
3	17	0	100
4	18	90	10

Method C

Step	Time / min	% H_2O	% MeCN
0	0	90	10
1	0.5	90	10
2	11.5	0	100
3	15	0	100
4	16	90	10

Method D

Step	Time / min	% H_2O	% MeOH
0	0	90	10
1	7	0	100
2	12	0	100
3	14	90	100

Method E

Step	Time / min	% H_2O	% MeOH
0	0	90	10
1	3	90	10
2	13	0	100
3	18	0	100
4	20	90	10

Synthesis of [Ln.L^2]

The synthesis of the target pyridyl arm was achieved with the synthetic route described in Scheme 2.1. Adapted from a literature procedure (T. W. Bell, L. Y. Hu and S. V. Patel, J. Am. Chem. Soc., 1987, 52, 3847.), the first step involved a copper(I) catalysed Grignard reaction to introduce the *iso*-propyl group onto the 4-position of the pyridine ring in reasonable yield. Subsequent oxidation of **1** using *m*CPBA gave the N-oxide product **2**. Cyanation in the *ortho* position was achieved with trimethylsilyl cyanide, through activation of the ring with dimethylcarbamyl chloride as the acylating electrophile to afford **3**. Direct cyanation using KCN as the strong nucleophilic cyanide source was attempted without any prior activation of the pyridine ring and did not proceed. Transformation of the nitrile group into the corresponding methyl ester product **5** proceeded via base hydrolysis to the carboxylic acid **4** before the acid catalysed esterification step. Direct conversion of **3** to the methyl ester derivative **5** was attempted via methanolysis of the nitrile group by heating in a solution of MeOH and concentrated H_2SO_4. The formation of the protonated methyl amide intermediate was observed by mass spectrometry. However, efforts to isolate **5** by treating the intermediate with water saw full conversion back to **3**. A second N-oxidation yielded **6**, which underwent a [3,3]-sigmatropic rearrangement upon heating with trifluoroacetic anhydride. The trifluoroacetate ester intermediate was identified by ^{1}H and ^{19}F NMR spectroscopy before treatment with a 1:1 mixture of ethanol and water afforded the alcohol **7**. Reaction with methanesulfonyl chloride and triethylamine as the base gave the mesylate **8**.

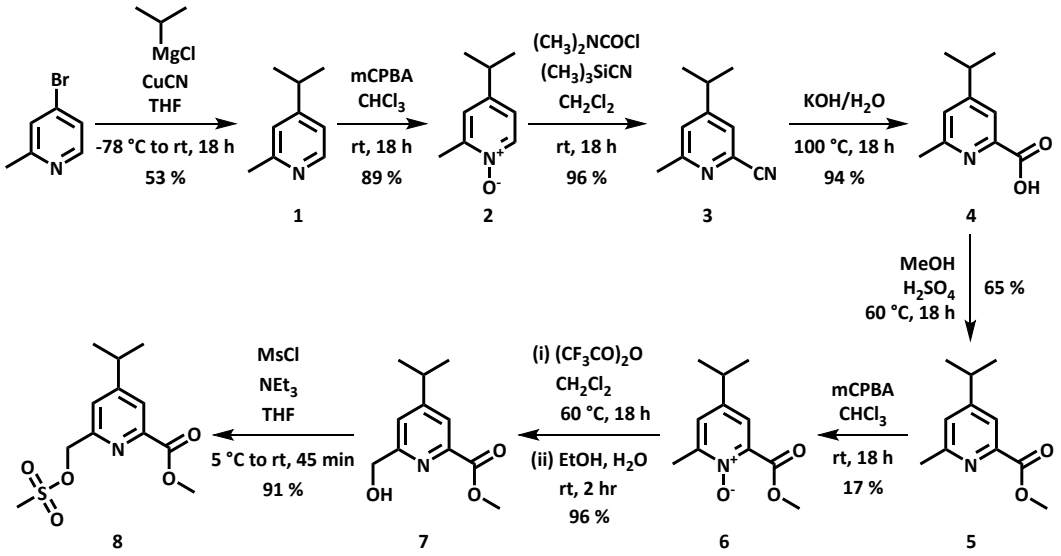

Scheme S1 General procedure for the synthesis of the *iso*-propyl substituted $\mathbf{L^2}$ ligand.

The 9-N_3 macrocycle was alkylated immediately with the mesylated pyridyl arm using the base, Cs_2CO_3 and a non-protic solvent, in this case MeCN, to avoid decomposition of **8**. Base hydrolysis removed the methyl protecting groups and the resulting deprotected ligand was used for complexation in aqueous solution at pH 6.5 to yield the desired lanthanide complex, [LnL^2] where Ln = Yb, Tb and Eu (**10** – **12**), and the analogous diamagnetic derivative, [YL^2] (**13**), subjected to further purification by preparative reversed-phase HPLC.

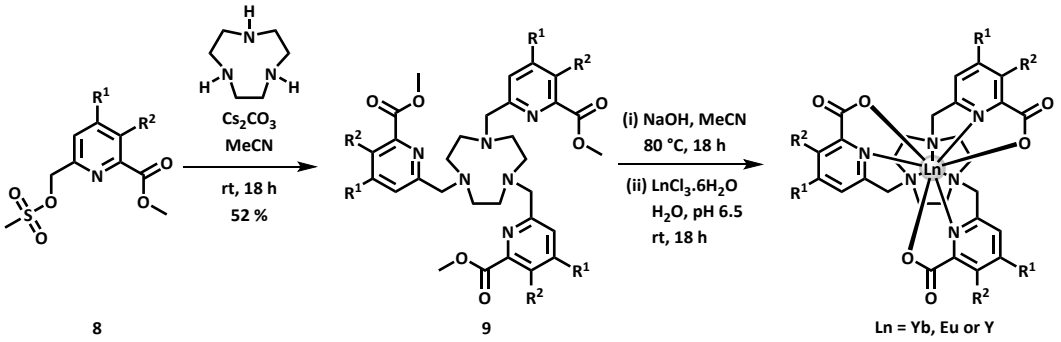

Scheme S2 General procedure for the formation of [$Ln.L^2$] and [$Y.L^2$].

4-*iso*-Propyl-2-methylpyridine 1

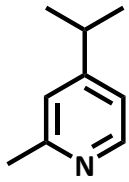

Copper(I) cyanide (30 mg) was added to anhydrous THF (100 mL) under argon and the resulting suspension was cooled to -78 °C. *iso*-Propylmagnesium chloride (58 mL, 2.0 M in Et_2O, 116 mmol) was added and the mixture was stirred. The conditions were maintained for a further 20 min before 4-bromo-2-methylpyridine (10.0 g, 58.1 mmol) was added. The resulting orange solution was then allowed to warm to rt and stirred for a further 18 h. NH_4OH (sat. aq. solution, 25 mL) was added dropwise to the red solution. The green precipitate was filtered and THF was removed under reduced pressure from the resulting yellow filtrate. The aqueous layer was then extracted with Et_2O (3 x 50 mL), dried over $MgSO_4$ and the solvent was removed under reduced pressure. The resulting orange liquid was purified by silica gel column chromatography, eluting with a gradient starting from 15% EtOAc/hexane to 40% EtOAc/hexane, to yield a pale yellow oil (4.13 g, 53%). ^{1}H NMR (700 MHz, $CDCl_3$) δ 8.35 (1H, d, ^3J 5.2, H^6), 6.98 (1H, s, H^3), 6.93 (1H, d, ^3J 5.2, H^5), 2.82 (1H, sep, ^3J 7.0, C*H*$(CH_3)_2$), 2.51 (3H, s, C*H*$_3$) 1.22 (6H, d, ^3J 7.0, CH(C*H*$_3)_2$); ^{13}C NMR (176 MHz, $CDCl_3$) δ 158.2 (C^2), 157.9 (C^4), 148.9 (C^6), 121.5 (C^3), 119.1 (C^5), 33.5 (*C*H$(CH_3)_2$), 24.3 (*C*H$_3$), 23.1 (CH(*C*H$_3)_2$); ESI-HRMS (+) calcd for $[C_9H_{14}N]^+$ 136.1126, found 136.1112 $[M+H]^+$.

4-*iso*-Propyl-2-methylpyridin-1-oxide 2

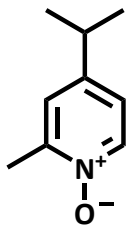

*m*CPBA (8.41 g, 48.7 mmol) was added to a solution of 4-*iso*-propyl-6-methylpyridine (4.13 g, 30.5 mmol) in anhydrous $CHCl_3$ (130 mL). The resulting solution was stirred at rt for 18 h under argon, before quenching with Na_2SO_4 (sat. aq. solution, 30 mL) and stirring for a further 10 min. The organic layer was extracted and washed with NaOH (0.8 M, 3 x 50 mL) and H_2O (2 x 50 mL). The aqueous layer was then extracted with CH_2Cl_2 (3 × 100 mL). The organic layers were combined, dried over $MgSO_4$ and the solvent removed under reduced pressure to yield a pale yellow liquid (4.13 g, 89%). ^{1}H NMR (700 MHz, $CDCl_3$) δ 8.15 (1H, d, ^3J 6.7, H^6), 7.06 (1H, d, ^4J 2.6, H^3), 6.96 (1H, dd, ^3J 6.7, ^4J 2.6, H^5), 2.84 (1H, sep, ^3J 7.0, C*H*$(CH_3)_2$), 2.48 (3H, s, C*H*$_3$), 1.21 (6H, d, ^3J 7.0, CH(C*H*$_3)_2$) ; ^{13}C NMR (176 MHz,

$CDCl_3$) δ 148.4 (C^2), 147.6 (C^4), 138.9 (C^6), 124.5 (C^3), 121.6 (C^5), 32.8 ($CH(CH_3)_2$), 23.0 ($CH(CH_3)_2$), 17.9 (CH_3); ESI-HRMS (+) calcd for $[C_9H_{14}NO]^+$ 152.1075, found 152.1067 $[M+H]^+$.

2-Cyano-4-*iso*-propyl-6-methylpyridine 3

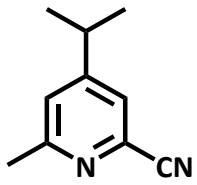

Trimethylsilyl cyanide (2.1 mL, 16.8 mmol) was added dropwise to a stirred solution of 4-*iso*-propyl-6-methylpyridin-1-oxide (1.76 g, 11.7 mmol) in dry CH_2Cl_2 (15 mL) under argon. After 15 minutes, dimethyl carbamyl chloride (0.70 mL, 16.3 mmol) in dry CH_2Cl_2 (5.0 mL) was added and the resulting mixture was stirred at rt for 18 h. K_2CO_3 (10% aq. solution, 20 mL) was added and the aqueous layer was extracted with CH_2Cl_2 (3 x 30 mL). The combined organic phase was then washed with water (2 x 30 mL), dried over $MgSO_4$ and the solvent removed under reduced pressure. The resulting yellow liquid was purified by silica gel column chromatography, eluting with 5% EtOAc/hexane to yield a colourless oil (1.79 g, 96%). ^{1}H NMR (700 MHz, $CDCl_3$) δ 7.36 (1H, dd, ^4J 1.7, 0.6, H^3), 7.19 (1H, dd, ^4J 1.7, 0.6, H^5), 2.89 (1H, sep, ^3J 7.0, $CH(CH_3)_2$), 2.56 (3H, s, CH_3), 1.25 (6H, d, ^3J 7.0, $CH(CH_3)_2$); ^{13}C NMR (176 MHz, $CDCl_3$) δ 160.5 (C^6), 159.1 (C^4), 133.2 (CN), 125.1 (C^5), 124.3 (C^3), 117.7 (C^2), 33.4 ($CH(CH_3)_2$), 24.3 (CH_3), 22.8 ($CH(CH_3)_2$); ESI-HRMS (+) calcd for $[C_{10}H_{13}N_2]^+$ 161.1079, found 161.1071 $[M+H]^+$.

4-*iso*-Propyl-6-methylpyridin-2-carboxylic acid 4

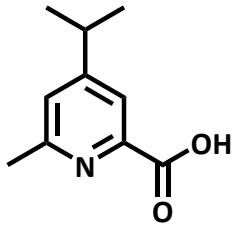

2-Cyano-4-*iso*-propyl-6-methylpyridine (1.43 g, 8.93 mmol) was added to a solution of KOH (1M, 20 mL). The resulting solution was allowed to reflux at 100 °C for 18 h before cooling to rt and acidified with a mixture of conc. H_2SO_4 (aq, 1 mL) diluted in H_2O (4 mL). The solvent was removed under reduced pressure to yield a colourless oil (1.51 g, 94%). ^{1}H NMR (600 MHz, D_2O) δ 8.21 (1H, d, ^4J 1.8, H^3), 7.88 (1H, d, ^4J 1.8, H^5), 3.19 (1H, sep, ^3J 6.9, $CH(CH_3)_2$), 2.76 (3H, s, CH_3), 1.28 (6H, d, ^3J 6.9, $CH(CH_3)_2$); ^{13}C NMR (151 MHz, D_2O) δ 170.9 (CO), 162.2 (C^4), 154.8 (C^6), 140.6 (C^2), 128.7 (C^5), 123.6 (C^3), 34.2 ($CH(CH_3)_2$), 21.4 ($CH(CH_3)_2$), 18.8 (CH_3); ESI-HRMS (+) calcd for $[C_{10}H_{14}NO_2]^+$ 180.1025, found 180.1015 $[M+H]^+$.

Methyl 4-*iso*-propyl-6-methylpyridin-2-carboxylate 5

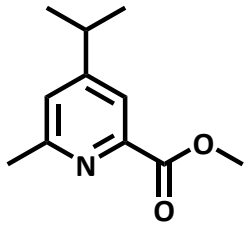

4-*iso*-Propyl-6-methylpyridin-2-carboxylic acid (1.51 g, 8.43 mmol) was dissolved in dry methanol (10 mL) and to this was added 5 drops of conc. H_2SO_4 (aq). The resulting solution was allowed to reflux at 60 °C for 18 h before neutralising with K_2CO_3 (sat. aq. solution). The aqueous phase was extracted with hexane (2 x 15 mL). The organic layers were combined, dried over $MgSO_4$ and the solvent was removed under reduced pressure to yield a colourless liquid (1.06 g, 65%). ^{1}H NMR (700 MHz, $CDCl_3$) δ 7.79 (1H, d, ^4J 1.5, H^3), 7.14 (1H, d, ^4J 1.5, H^5), 3.94 (3H, s, COOCH_3), 2.88 (1H, sep, ^3J 6.9, CH(CH$_3$)$_2$), 2.58 (3H, s, CH_3), 1.22 (6H, d, ^3J 6.9, CH(CH_3)$_2$); ^{13}C NMR (176 MHz, $CDCl_3$) δ 166.3 (*C*O), 159.0 (C^4), 158.9 (C^6), 147.5 (C^2), 125.0 (C^5), 121.0 (C^3), 52.8 (COO*C*H$_3$), 33.5 (*C*H(CH$_3$)$_2$), 24.6 (*C*H$_3$), 23.0 (CH(*C*H$_3$)$_2$); ESI-HRMS (+) calcd for $[C_{11}H_{16}NO_2]^+$ 194.1181, found 194.1178 $[M+H]^+$

2-(Methoxycarbonyl)-4-*iso*-propyl-6-methylpyridin-1-oxide 6

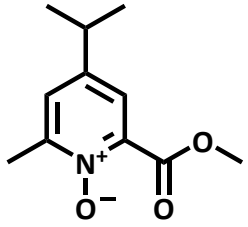

*m*CPBA (1.51 g, 8.75 mmol) was added to a stirred solution of methyl 4-*iso*-propyl-6-methylpyridin-2-carboxylate (1.06 g, 5.49 mmol) in anhydrous CHCl3 (40 mL). The resulting solution was stirred at rt for 18 h under argon, before quenching with Na_2SO_4 (sat. aq. solution, 10 mL) and stirring for a further 10 min. The organic layer was extracted and washed with NaOH (0.8 M, 2 x 20 mL) and H_2O (2 x 10 mL). The aqueous layer was then extracted with CH_2Cl_2 (3 × 10 mL). The organic layers were combined, dried over $MgSO_4$ and the solvent removed under reduced pressure. The resulting orange oil was purified by silica gel column chromatography, eluting with a gradient starting from 100% CH_2Cl_2 to 3% MeOH/CH_2Cl_2, to yield a pale yellow oil (0.19 g, 17%). ^{1}H NMR (700 MHz, $CDCl_3$) δ 7.25 (1H, d, ^4J 2.7, H^3), 7.16 (1H, d, ^4J 2.7, H^5), 3.99 (3H, s, COOCH_3), 2.87 (1H, sep, ^3J 6.9, CH(CH$_3$)$_2$), 2.51 (3H, s, CH_3), 1.24 (6H, d, ^3J 6.9, CH(CH_3)$_2$); ^{13}C NMR (176 MHz, $CDCl_3$) δ 163.1 (*C*O), 149.8 (C^6), 146.5 (C^4), 141.4 (C^2), 125.8 (C^5), 121.8 (C^3), 53.2 (COO*C*H$_3$), 32.9 (*C*H(CH$_3$)$_2$), 23.0 (CH(*C*H$_3$)$_2$), 17.8 (*C*H$_3$); ESI-HRMS (+) calcd for $[C_{11}H_{16}NO_3]^+$ 210.1130, found 210.1138 $[M+H]^+$.

Methyl 4-*iso*-propyl-6-(hydroxymethyl)pyridin-2-carboxylate 7

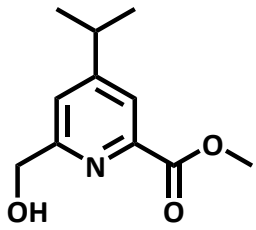

Trifluoroacetic anhydride (0.80 mL, 5.72 mmol) was added to a solution of 2-(methoxycarbonyl)-4-*iso*-propyl-6-methylpyridin-1-oxide (0.17 g, 0.812 mmol) in CH_2Cl_2 (5 mL). The resulting mixture was heated at 60 °C for 18 h under argon. Reaction completion was confirmed by ^1H and ^{19}F NMR spectroscopy. The solvent was then removed under reduced pressure. The resulting bright yellow oil was stirred in a mixture of EtOH (5 mL) and H_2O (5 mL) at rt for 2 h. The solution was concentrated (*ca.* 5 mL) and extracted with CH_2Cl_2 (3 × 20 mL), before the organic layers were combined, dried over $MgSO_4$, and the solvent removed under reduced pressure to yield a pale yellow oil (0.76 g, 96%). ^1H NMR (700 MHz, $CDCl_3$) δ 7.89 (1H, d, ^4J 1.7, H^3), 7.36 (1H, d, ^4J 1.7, H^5), 4.82 (2H, s, CH_2OH), 3.97 (3H, s, COOCH_3), 2.97 (1H, sep, ^3J 7.0, CH(CH_3)$_2$), 1.28 (6H, d, ^3J 7.0, CH(CH_3)$_2$); ^{13}C NMR (176 MHz, $CDCl_3$) δ 165.9 (*C*O), 160.1 (C^6), 159.8 (C^4), 147.1 (C^2), 122.5 (C^3), 122.1 (C^5), 64.7 (*C*H_2OH), 52.8 (COO*C*H_3), 33.7 (*C*H(CH_3)$_2$), 23.0 (CH(*C*H_3)$_2$); ESI-HRMS (+) calcd for $[C_{11}H_{16}NO_3]^+$ 210.1130, found 210.1135 $[M+H]^+$.

Methyl 4-*iso*-propyl-6-[(methanesulfonyloxy)methyl]pyridin-2-carboxylate 8

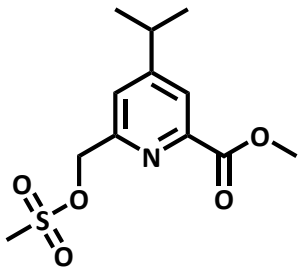

Triethylamine (0.42 mL, 3.01 mmol) was added to a solution of methyl 4-*iso*-propyl-6-(hydroxymethyl)pyridin-2-carboxylate (0.16 g, 0.764 mmol) in anhydrous THF (5 mL) and the resulting solution was cooled in ice. Methanesulfonyl chloride (0.09 mL, 1.16 mmol) was added dropwise and the resulting suspension was allow to stir at rt under argon. Complete consumption of starting material was confirmed by silica TLC after 45 min. The solvents were removed under reduced pressure and the residue was treated with H_2O (2 x 5 mL). The aqueous solution was extracted with CH_2Cl_2 (3 x 5 mL). The organic layers were combined, dried over $MgSO_4$, and the solvent removed under reduced pressure to yield an orange oil, which was used immediately without further purification (0.20 g, 91%). ^1H NMR (400 MHz, $CDCl_3$)

δ 7.99 (1H, d, ^4J 1.6, H^3), 7.52 (1H, d, ^4J 1.6, H^5), 5.41 (2H, s, CH_2), 4.00 (3H, s, COOCH_3), 3.15 (3H, s, CH_3), 3.02 (1H, sep, ^3J 6.9, CH(CH_3)$_2$), 1.31 (6H, d, ^3J 6.9, CH(CH_3)$_2$); ESI-HRMS (+) calcd for $[C_{12}H_{18}NO_5S]^+$ 288.0906, found 288.0914 $[M+H]^+$.

1,4,7-Tris({4-*iso*-propyl-6-[methoxycabonyl]-pyridin-2-yl}methyl)-1,4,7-triazacyclonane (trimethyl ester of L^2), 9

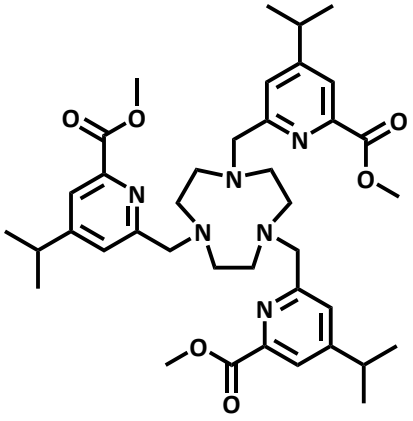

Methyl 4-*iso*-propyl-6-[(methanesulfonyloxy)methyl]pyridin-2-carboxylate (190 mg, 0.661 mmol) was added dropwise as a solution in dry MeCN (3 mL) to a mixture of 1,4,7-triazacyclononane trihydrochloride (48 mg, 0.604 mmol) and Cs_2CO_3 (395 mg, 1.21 mmol) in anhydrous MeCN (2 mL). The resulting mixture was stirred at 60 °C for 18 h under argon before allowing to cool to rt. The yellow solution was decanted from insoluble salts after centrifugation and then purified by alumina gel column chromatography, eluting with a gradient starting from 100% CH_2Cl_2 to 2% MeOH/CH_2Cl_2, to yield a yellow oil (73 mg, 52%). ^{1}H NMR (600 MHz, $CDCl_3$) δ 7.81 (3H, s, H^3), 7.60 (3H, s, H^5), 3.99 (6H, br s, CH_2), 3.88 (9H, s, COOCH_3), 2.98 (12H, br s, ring CH_2), 2.89 (1H, sep, ^3J 6.9, CH(CH_3)$_2$), 1.25 – 1.14 (18H, m, CH(CH_3)$_2$); ^{13}C NMR (151 MHz, $CDCl_3$) δ 125.0 (C^5), 122.4 (C^3), 63.6 (br, CH$_2$), 54.9 (br, ring CH$_2$), 33.6 (CH(CH_3)$_2$), 23.0 (CH(CH$_3$)$_2$); ESI-HRMS (+) calcd for $[C_{39}H_{55}N_6O_6]^+$ 703.4183, found 703.4193 $[M+H]^+$.

[Yb.L^2] Aqueous sodium hydroxide solution (0.17 M, 1 mL) was added to a solution of the trimethyl ester of **L^2** (24 mg, 34.6 μmol) in MeCN (1 mL). The mixture was stirred at 80 °C for 18 h until complete ester hydrolysis was confirmed by ESI-LRMS (+) (*m/z* 661.98 $[M+H]^+$; ESI-HRMS (+) calcd for $[C_{36}H_{49}N_6O_6]^+$ 661.3714, found 661.3726). HCl (aq, 0.1 M) was added to the solution until pH 6.5 was achieved. $YbCl_3.6H_2O$ (15 mg, 38.7 μmol) was then added and the pH was readjusted to 6.5 by the addition of NaOH (aq, 0.1 M). The reaction mixture was stirred at rt for 18 h. The pH was further increased to 11

and the yellow solution was decanted from insoluble salts after centrifugation. The solvent was removed under reduced pressure and the resulting pale yellow solid was purified by reverse-phase HPLC (Waters X-Bridge C18, method A) to yield **[Yb.L^2]** as a white solid (t_R = 8.3 min, 17 mg). ESI-HRMS (+) calcd for $[YbC_{36}H_{46}N_6O_6]^+$ 828.2827, found 832.2856 $[M+H]^+$.

[Y.L^2]

An analogous procedure to that described for the synthesis of **[Yb.L^2]** was followed using the trimethyl ester of **L^2** (13.9 mg, 19.8 μmol) and YCl_3 (8 mg, 41.0 μmol) to yield a white solid (t_R = 8.3 min, 8 mg); ^{1}H NMR (600 MHz, MeCN-d_3) δ 7.89 (3H, s, H^3), 7.44 (3H, s, H^5), 3.99 (3H, d, ^2J 14.0, py-C*H*N (pro-R)), 3.88 (3H, d, ^2J 14.0, py-C*H*N (pro-S)), 3.39 (3H, td, ^2J 16.3, ^3J 4.9, H^{ax}), 3.11 (3H, sep, ^3J 6.9, C*H*(CH$_3$)$_2$), 2.70 (3H, dd, ^2J 16.3, ^3J 5.6, H^{eq}), 2.48 (3H, dd, ^2J 12.9, ^3J 4.9, H$^{eq'}$), 2.23 (3H, td, ^2J 12.9, ^3J 4.9, H$^{ax'}$), 1.32 (18H, d, ^3J 6.9, CH(C*H*$_3$)$_2$); ^{13}C NMR (151 MHz, $CDCl_3$) δ 122.5 (C^5), 121.0 (C^3), 65.3 (py-*C*HN), 57.6 (*C*H$^{ax'}$ and *C*H$^{eq'}$), 54.7 (*C*H^{ax} and *C*H^{eq}), 33.7 (*C*H(CH$_3$)$_2$), 22.3 and 22.2 (CH(*C*H$_3$)$_2$); ESI-HRMS (+) calcd for $[C_{39}H_{55}N_6O_6]^+$ 703.4183, found 703.4193 $[M+H]^+$; ESI-HRMS (+) calcd for $[YC_{36}H_{46}N_6O_6]^+$ 747.2537, found 747.2530 $[M+H]^+$.

[Eu.L^2]

An analogous procedure to that described for the synthesis of **[Yb.L^2]** was followed using the trimethyl ester of **L^2** (24 mg, 34.6 μmol) and $EuCl_3.6H_2O$ (15 mg, 40.9 μmol) to yield a white solid (t_R = 8.3 min, 15 mg). ESI-HRMS (+) calcd for $[EuC_{36}H_{46}N_6O_6]^+$ 809.2677, found 809.2676 $[M+H]^+$

Synthesis of [Ln.L^3]

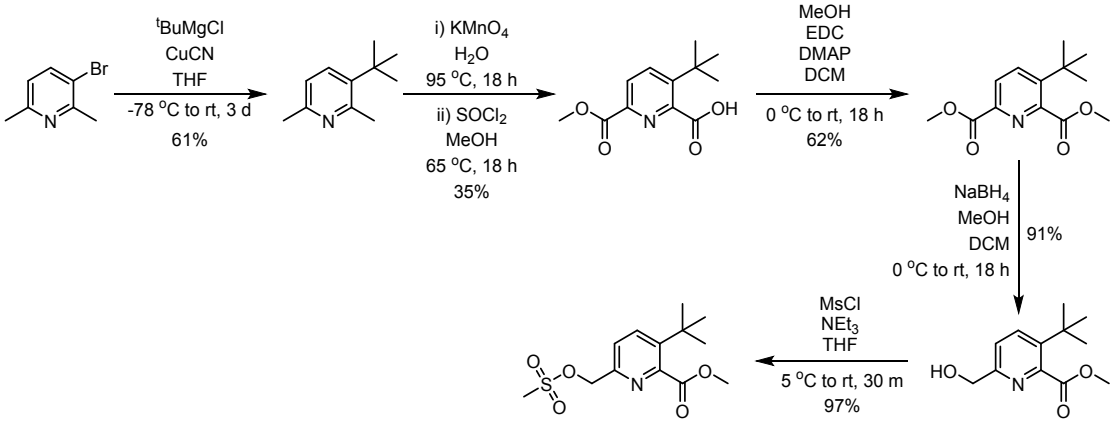

Scheme S3

3-*tert*-butyl-2,6-dimethylpyridine

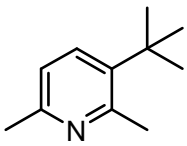

Copper(I) cyanide (20 mg) was suspended in THF (150 mL) under argon. The resulting suspension was cooled to -78 °C before *tert*-butylmagnesium chloride (27 mL, 2.0 M in Et_2O, 54 mmol) was added. 3-Bromo-2,6-dimethylpyridine (5.0 g, 26.9 mmol) was added and the resulting yellow solution was allowed to warm to rt and then heated to 50 °C stirred for a further 18 h. NH_4OH (sat. aq. solution, 20 mL) was added dropwise to the resulting red solution. The resulting suspension was filtered and the solid was washed with Et_2O (3 x 200 mL). The organic layers were combined and dried over $MgSO_4$. The solvent was removed under reduced pressure to yield an orange liquid that was purified by silica gel column chromatography, eluting with a gradient starting from 100% hexane to 5% EtOAc/ hexane to yield a yellow liquid (2.68 g, 61%). R_f (20% EtOAc/ hexane) = 0.43. ^{1}H NMR (700 MHz,$CDCl_3$) δ 7.42 (d, ^3J = 8, 1H, H^4), 6.80 (d, ^3J = 8, 1H, H^5), 2.63 (s, 3H, C^{2}H$_3$), 2.38 (s, 3H, C^{6}H$_3$), 1.30 (s, 9H, C(C$\underline{H}_3$)$_3$); ^{13}C NMR (176 MHz, $CDCl_3$) δ 155.8 (C^2), 154.1 (C^6), 139.9 (C^3), 134.0 (C^4), 120.2 (C^5), 34.1 (C(CH$_3$)$_3$), 30.5 (C($\underline{C}$H$_3$)), 26.1 (C^{2}H$_3$), 23.6 (C^{6}H$_3$); ESI-LRMS (+) *m/z* 164.8 [M+H]$^+$; ESI-HRMS (+) calcd for [$C_{11}H_{18}N$]$^+$ 164.1439, found 164.1448.

6-(Methoxycarbonyl)-3-*tert*-butylpyridine-2-carboxylic acid

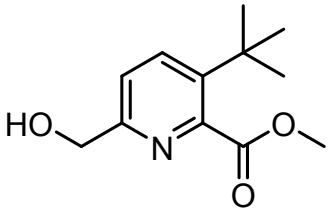

3-*tert*-butyl-2,6-dimethylpyridine (3 g, 18.4 mmol) was added to H_2O (150 mL) and the two immiscible

layers were stirred at 95°C for 10 min. $KMnO_4$ (14.5 g, 92 mmol) was added and the reaction was stirred at 95°C for 18 h. The resulting suspension was allowed to cool to rt and filtered over celite. The solvent was removed under reduced pressure to yield an off white solid that was used without further purification (LRMS (+) *m/z* 223.9 $[M+H]^-$; ESI-HRMS (+) calcd for $[C_{11}H_{14}NO_4]^+$ 224.0923, found 224.0928). The salt was suspended in anhydrous MeOH (40 mL) and the suspension was cooled to 0°C. Thionyl chloride (13 mL, 180 mmol) was added dropwise and the reaction was heated at 65°C for 18 h, after which the solvent was removed under reduced pressure. The resulting yellow oil was purified by silica gel column chromatography, eluting with a gradient starting from 100% CH_2Cl_2 to 5% MeOH/ CH_2Cl_2 to yield a yellow (1.53 g, 35%). R_f (5% MeOH/ CH_2Cl_2) = 0.16; ^{1}H NMR (700 MHz, $CDCl_3$) δ 8.04 (d, ^3J = 8.5, 1H, H^5), 7.97 (d, ^3J = 8.5, 1H, H^4), 3.93 (s, 3 H, CO_2CH_3), 1.41 (s, 9H, $C(C\underline{H}_3)_3$); ^{13}C NMR (176 MHz, $CDCl_3$) δ 169.1 (CO_2H), 164.9 ($\underline{C}O_2CH_3$), 150.1 (C^2), 148.2 (C^3), 143.4 (C^6), 137.2 (C^4), 125.8 (C^5), 53.0 (OCH_3), 35.2 ($\underline{C}(CH_3)_3$), 30.6 ($C(\underline{C}H_3)$); ESI-LRMS (+) *m/z* 238.4 $[M+H]^+$; ESI-HRMS (+) calcd for $[C_{12}H_{16}NO_4]^+$ 238.1079, found 238.1070.

Dimethyl 3-*tert*-butyl-2,6-pyridinecarboxylate was also isolated from the column as a yellow oil (1.07 g, 23%). R_f (5% MeOH/ CH_2Cl_2) = 0.89; ESI-LRMS (+) *m/z* 252.0 $[M+H]^+$.

Dimethyl 3-*tert*-butyl-2,6-pyridinecarboxylate

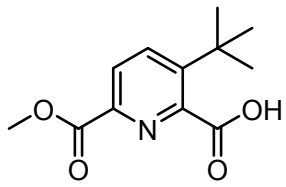

6-(Methoxycarbonyl)-3-tert-butylpyridine-2-carboxylic acid (2.7 g, 11.4 mmol) was dissolved in a solution of anhydrous DCM (20 mL) and anhydrous MeOH (1 mL) and stirred at 0°C under argon. N-(3-Dimethylaminopropyl)-N′-ethylcarbodiimide hydrochloride (EDC) (3.72 g, 19.38 mmol) and DMAP (280 mg, 2.28 mmol) were added and the reaction mixture was allowed to warm to rt. The solution was stirred for 18h and then was washed with water (3 x 50 mL). The organic layer was dried with $MgSO_4$ before the solvent was removed under reduced pressure. The resulting yellow oil was purified by silica gel column chromatography, eluting with a gradient starting from 100% CH_2Cl_2 to 1% MeOH/ CH_2Cl_2 to yield a pale yellow oil (1.78 g, 62%). R_f (5% MeOH/ CH_2Cl_2) = 0.87; ^{1}H NMR (700 MHz, $CDCl_3$) δ 8.10 (d, ^3J = 8.5, 1H, H^5), 7.96 (d, ^3J = 8.5, 1H,

H[4]), 3.97 (s, 6H, OCH_3), 1.41 (s, 9H, $C(C\underline{H}_3)_3$); ^{13}C NMR (176 MHz, $CDCl_3$) δ 168.8 ($C^2\underline{C}O_2CH_3$), 165.3 ($C^6\underline{C}O_2CH_3$), 150.7 (C^2), 146.9 (C^3), 144.8 (C^6), 136.6 (C^4), 125.8 (C^5), 53.1 (OCH_3), 53.0 (OCH_3), 35.1 ($\underline{C}(CH_3)_3$), 30.9 ($C(\underline{C}H_3)$); ESI-LRMS (+) *m/z* 252.0 $[M+H]^+$; ESI-HRMS (+) calcd for $[C_{13}H_{18}NO_4]^+$ 252.1236, found 252.1227.

Methyl 6-hydroxymethyl-3-*tert*-butyl-2-pyridinecarboxylate

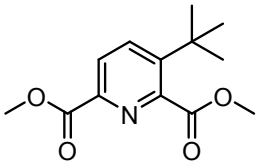

Dimethyl 3-*tert*-butyl-2,6-pyridinecarboxylate (500 mg, 1.98 mmol) was dissolved in a solution of anhydrous DCM (2 mL) and anhydrous MeOH (2 mL) and stirred at 0°C. $NaBH_4$ (166 mg, 4.4 mmol) was added and the reaction was stirred at 0°C for 30 min after which it was allowed to warm to rt and stirred for a further 1 h. The solution was then cooled to 0°C before the addition of DCM (2 mL) and 1M HCl (2 mL) to quench the reaction. The mixture was washed with water (5 mL) and the organic layer was dried with $MgSO_4$ before the solvent was removed under reduced pressure. The resulting yellow oil was purified by silica gel column chromatography, eluting with a gradient starting from 100% CH_2Cl_2 to 2% MeOH/ CH_2Cl_2 to yield a pale yellow oil (424 mg, 96%). R_f (5% MeOH/ CH_2Cl_2) = 0.47; ^1H NMR (700 MHz, $CDCl_3$) δ 7.78 (d, ^3J = 8.5, 1H, H^4), 7.29 (d, ^3J = 8.5, 1H, H^5), 4.69 (s, 2H, CH_2OH), 3.91 (s, 3 H, CO_2CH_3), 1.34 (s, 9H, $C(C\underline{H}_3)_3$); ^{13}C NMR (176 MHz, $CDCl_3$) δ 169.7 ($\underline{C}O_2CH_3$), 156.3 (C^6), 149.0 (C^2), 141.2 (C^3), 136.3 (C^4), 121.3 (C^5), 64.0 (CH_2OH), 52.7 (OCH_3), 34.3 ($\underline{C}(CH_3)_3$), 31.0 ($C(\underline{C}H_3)$); ESI-LRMS (+) *m/z* 223.8 $[M+H]^+$; ESI-HRMS (+) calcd for $[C_{12}H_{18}NO_3]^+$ 224.1287, found 224.1266.

Methyl 6-([methanesulfonyloxy]methyl)-3-*tert*-butyl-2-pyridinecarboxylate

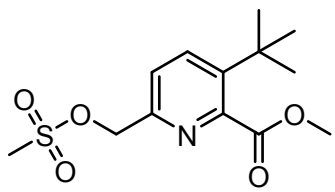

(3-*tert*-butyl-6-(tetrahydropyran-2-yloxymethyl)-pyridin-2yl) methanol (224 mg, 1 mmol) was dissolved in anhydrous THF (4 mL) and stirred at 5°C for 10 min, before the addition of NEt_3 (250 µL, 1.8 mmol). Mesyl chloride (90 µL, 1.15 mmol) was added dropwise and the resulting solution was allowed to stir at rt for 30 min. The solvent was removed under

reduced pressure and the residue was dissolved in H_2O (5 mL) and extracted with CH_2Cl_2 (3 x 10 mL). The organic layers were combined and dried over $MgSO_4$ and the solvent removed under reduced pressure. The resulting yellow oil was used immediately (293 mg, 97 %). R_f (5% MeOH/ CH_2Cl_2) = 0.81; ^{1}H NMR (400 MHz, $CDCl_3$) δ 7.85 (d, ^3J = 8.5, 1H, H^4), 7.44 (d, ^3J = 8.5, 1H, H^5), 5.25 (s, 2H, CH_2OMs), 3.90 (s, 3H, CO_2CH_3), 3.04 (s, 3H, CH_3) 1.33 (s, 9H, $C(C\underline{H}_3)_3$); ESI-LRMS (+) *m/z* 302.6 $[M+H]^+$; ESI-HRMS (+) calcd for $[C_{13}H_{20}NO_5S]^+$ 302.1062, found 302.1062.

1,4,7-Tris(2-methoxycarbonyl-3-*tert*-butylpyridin-6-ylmethyl)- 1,4,7-triazacyclononane

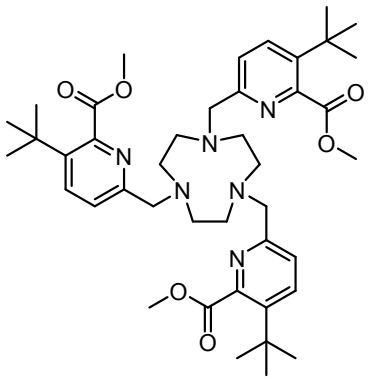

K_2CO_3 (110 mg, 0.8 mmol) and 1,4,7-triazacyclononane trihydrochloride (40 mg, 0.17 mmol) was suspended in anhydrous MeCN (1 mL). Methyl 6-([methanesulfonyloxy]methyl)-3-*tert*-butyl-2-pyridinecarboxylate (170 mg, 0.54 mmol) was then added dropwise as a solution in anhydrous MeCN (2 mL). The resulting solution was heated to 70°C and stirred for 18 h before being cooled to rt and filtered to remove inorganic salts. The solvent was removed under reduced pressure and the resulting orange oil was purified by silica gel column chromatography, eluting with a gradient starting from 100% CH_2Cl_2 to 1% MeOH/ CH_2Cl_2 to yield a yellow oil (60 mg, 47 %). R_f (5% MeOH/ CH_2Cl_2) = 0.76; ^{1}H NMR (600 MHz, $CDCl_3$) δ 7.76 (d, ^3J = 8.5, 3H, H^4), 7.53 (d, ^3J = 8.5, 3H, H^5), 3.92 (s, 9H, CO_2CH_3), 3.80 (s, 6H, NCH_2py), 2.86 (s, 12H, 9N3 CH_2), 1.35 (s, 27H, $C(CH_3)_3$). ^{13}C NMR (151 MHz, $CDCl_3$) δ 169.4 (CO), 151.9 (C^6), 150.1 (C^2), 142.61 (C^3), 136.7 (C^4), 124.9 (C^5), 59.0 (NCH_2py), 52.7 ($CO_2\underline{C}H_3$), 49.8 (9N3 CH_2), 34.5 ($\underline{C}(CH_3)_3$), 30.9 ($C(\underline{C}H_3)_3$); ESI-LRMS (+) *m/z* 745.7 $[M+H]^+$; ESI-HRMS (+) calcd for $[C_{42}H_{61}N_6O_6]^+$ 745.4653, found 745.4666.

Yttrium(III) complex of 1,4,7-Tris(2-methoxycarbonyl-3-*tert*-butylpyridin-6-ylmethyl)- 1,4,7-triazacyclononane [Y.L^3]

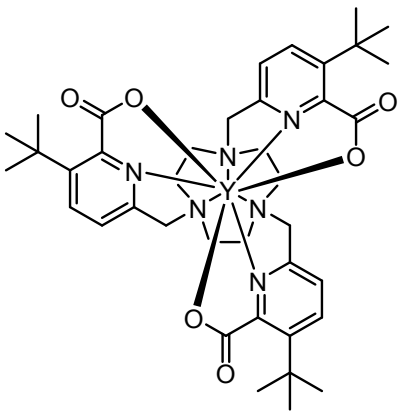

Aqueous sodium hydroxide solution (0.25 M, 1 mL) was added to a solution of 1,4,7-Tris(2-methoxycarbonyl-3-*tert*-butylpyridin-6-ylmethyl)- 1,4,7-triazacyclononane (14 mg, 0.019 mmol) in MeCN (1 mL) and stirred at 80°C for 18 h. Complete ester cleavage was confirmed by ESI-MS (+) (LR: *m/z* 676.6 $[M+H]^+$). The solvent was removed under reduced pressure to yield a yellow oil which was dissolved in H_2O. The pH of the resulting solution was adjusted to 5.5 using NaOH and $YCl_3 \cdot 6H_2O$ (11 mg, 0.037 mmol) was added. The solution was stirred at 70°C for 18 h before the solvent was removed under reduced pressure. The resulting yellow solid was purified by reverse-phase HPLC (Waters X-Bridge C18, method B) (t_R = 9.3 min) to yield a white solid (11 mg, 67%). ^{1}H NMR (600 MHz, CD_3OD) δ 8.16 (d, ^3J = 8.5, 3H, H^4), 7.50 (d, ^3J = 8.5, 3H, H^5), 4.16 (3H, d, ^2J = 14, NCH_2py (pro-R)), 3.98 (3H, d, ^2J = 14, NCH_2py (pro-S)), 3.52 (3H, m, H^{ax}), 2.75 (3H, dd, ^2J = 16.5, ^3J = 5.5, H^{eq}), 2.54 (3H, dd, ^2J = 13, ^3J = 5.5, $H^{eq'}$), 2.32 (3H, td, ^2J = 13, ^3J = 5.5, $H^{ax'}$), 1.55 (27H, s, $C(CH_3)_3$); ^{13}C NMR (151 MHz, CD_3OD) δ 173.7 (CO), 153.0 (C^6), 152.5 (C^2), 148.4 (C^3), 140.5 (C^4), 125.2 (C^5), 66.2 (NCH_2py), 59.1 ($\underline{C}H^{ax'}$ and $\underline{C}H^{eq'}$), 56.2 ($\underline{C}H^{ax}$ and CH^{eq}), 36.6 ($\underline{C}H(CH_3)_3$), 31.3 ($CH(\underline{C}H_3)_3$); ESI-LRMS (+) *m/z* 789.4 $[M-H]^+$; ESI-HRMS (+) calcd for $[C_{39}H_{52}N_6O_6Y]^+$ 789.3007, found 789.2996.

[Yb.L^3]

An analogous procedure to that described for the synthesis of [Y.L^3] was followed using 1,4,7-Tris(2-methoxycarbonyl-3-*tert*-butylpyridin-6-ylmethyl)-1,4,7-triazacyclononane (16 mg, 0.022 mmol) and $YbCl_3 \cdot 6H_2O$ (12 mg, 0.03 mmol), to yield a white solid (13 mg, 47%). ESI-LRMS (+) *m/z* 874.3 $[M+H]^+$. ESI-HRMS (+) calcd for $[C_{39}H_{52}N_6O_6Yb]^+$ 870.3296, found 870.3301.

[Eu.L^3]

An analogous procedure to that described for the synthesis of [Y.L^3] was followed using 1,4,7-Tris(2-methoxycarbonyl-3-*tert*-butylpyridin-6-ylmethyl)-1,4,7-triazacyclononane (13 mg, 0.017 mmol) and $EuCl_3 \cdot 6H_2O$ (7 mg, 0.02 mmol),

to yield a white solid (12 mg, 81%). ESI-LRMS (+) *m/z* 853.5 $[M+H]^+$. ESI-HRMS (+) calcd for $[C_{39}H_{52}N_6O_6Eu]^+$ 851.3147, found 851.3183.

Synthesis of LnL^4

Triethyl-6,6',6''-(1,4,7-triazacyclononane-1,4,7-triyl)tris(methylene))tris(4-nitropicolinate)

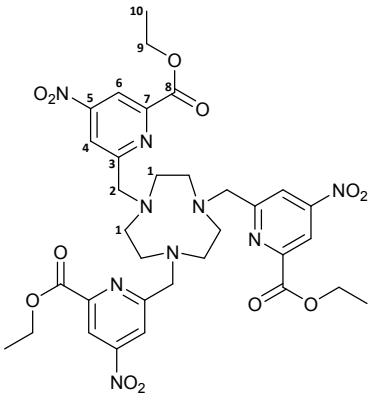

Ethyl-6-(((methylsulfonyl)oxy)methyl)-4-nitropicolinate (0.142 g, 0.5 mmol, 3.5 eq) was dissolved in anhydrous MeCN (3 mL) under argon. Triazacyclononane tri-hydrochloride (0.028 g, 0.1 mmol, 1 eq) and Cs_2CO_3 (0.233g, 0.7 mmol, 6.12 eq) were added to the mixture and heated to 60 °C with stirring for 14 h. A solid was removed by centrifugation, decanting the supernatant and rinsing the solid with MeCN and repeating. The organic layers were combined, and the solvent evaporated under reduced pressure. MeCN (2.5 mL) and water (2 mL) were added to dissolve and the crude product was purified by reverse phase HPLC (Waters X-Bridge C18, method C). The product fractions were combined, solvent evaporated and the residue taken up into DCM (2 x 20 mL). The combined organic layers were dried over Na_2SO_4 and solvent evaporated to yield an off-white solid (0.080 g, 0.1 mmol, 91%); ^{1}H NMR (400 MHz, $CHCl_3$) δ_H = 8.61 (d, 3H, *J* = 1.9 Hz), 8.56 (d, 3H, *J* = 1.9 Hz), 4.57 (s, 6H), 4.41 (q, 6H, *J* = 7.1 Hz), 3.44 (s, 12H), 1.40 (t, 9H, *J* = 7.1 Hz); ^{13}C NMR (126 MHz, $CDCl_3$) δ_C = 162.99 (C^5), 160.71 (C^8), 155.38 (C^3), 150.40 (C^7), 119.98 (C^6), 117.05 (C^4), 62.88 (C^9), 61.49 (C^2), 54.09 (C^1), 14.34 (C^{10}); HRMS$^+$: m/z = 754.2820 $[M+H]^+$ ($C_{33}H_{40}N_9O_{12}$ requires 754.2796).

6,6',6''-((1,4,7- Triazacyclononane -1,4,7-triyl)tris(methylene))tris(4-nitropicolinic acid)

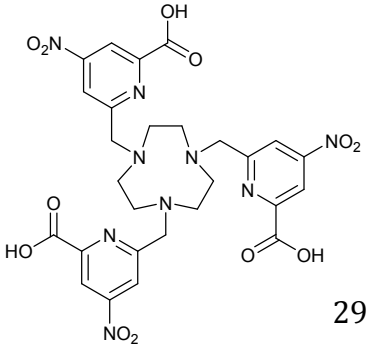

The ester-protected ligand (0.080 g, 0.1 mmol, 1 eq) was dissolved in MeCN (2 mL). KOH solution (0.2 M, 2.12 mL, 0.4 mmol, 4 eq) was added to the mixture and left to stir at rt for 6 h. The pH was returned to

7 and the solvent evaporated to yield a white solid in near quantitative yield; HRMS$^+$: m/z = 668.1711 [M-H]$^-$ ($C_{27}H_{26}N_9O_{12}$ requires 668.1701).

General Method for Complex Formation

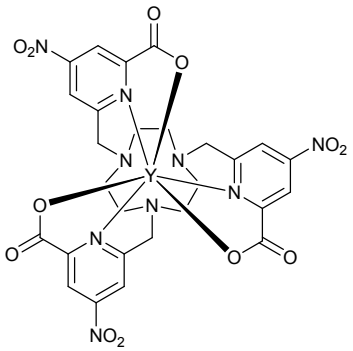

Deprotected ligand, L^6, (0.036 g, 53 μmol, 1 eq) was dissolved in MeCN (1 mL) and H_2O (1 mL). Anhydrous YCl_3 (0.014 g, 64 μmol, 1.2 eq) was added to ligand, the pH adjusted to 6 and left to stir for 2 h under Ar. The solid product was purified by centrifugation, where the supernatant was decanted and the solid washed with H_2O (3 × 1.5 mL). The solid was dried under reduced pressure to yield the Yttrium complex as a white solid (0.035 g, 46 μmol, 87%); ^{1}H NMR (700 MHz, d_6-DMSO) δ = 8.49 (d, 1H, *J* = 1.7 Hz), 8.41 (d, 1H, *J* = 1.7 Hz), 4.31 (d, 1H, *J* = 15.0 Hz), 4.04 (d, 1H, *J* = 15.0 Hz), 3.62 – 3.54 (m, 1H), 2.80 (dd, 1H, *J* = 16.4, 5.6 Hz), 2.56 – 2.47 (m, 1H), 2.31 – 2.25 (m, 1H); HRMS$^+$: m/z = 756.0681 [M+H]$^+$ ($C_{27}H_{25}N_9O_{12}Y$ requires 756.0692).

***p*-OMe Complex [Y.L^4]**

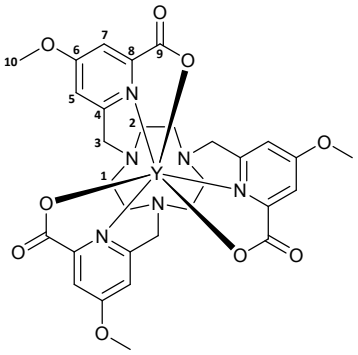

[**YL^6**] (0.035 g, 46 μmol, 1 eq) was dissolved in MeOH (1.5 mL) and H_2O (1.5 mL) and the pH adjusted to 7. Catalytic quantities of sodium metal (~ 50 mg) were dissolved in MeOH (1 mL), and the solution added to the complex mixture. The reaction was left stirring for at rt for 5 h under Ar. The pH was returned to 7 with HCl solution (1 M) and the solvent removed to yield crude [**Y.L^1**] as a solid. The solid was dissolved in MeOH (0.5 mL) and H_2O (4 mL) and purified by reverse phase HPLC (ACE C18-PFP, method D). Product fractions were combined and the solvent removed to yield [**Y.L^1**] as a white solid (0.030 g, 42 μmol, 80%); ^{1}H NMR (700 MHz, d_6-DMSO) δ 7.40 (d, 1H, *J* = 2.4 Hz), 7.20 (d, 1H, *J* = 2.4 Hz), 3.97 (s, 3H), 3.91 (d, 1H, *J* = 13.9 Hz), 3.77 (d, 1H, *J* = 13.9 Hz), 3.52 – 3.46 (m, 1H), 2.64 (dd, 1H, *J* = 16.2, 5.1 Hz), 2.45 (dd, 1H, *J* = 12.4, 5.1 Hz), 2.13 – 2.08 (m, 1H); ^{13}C NMR (176 MHz, d_6-DMSO) δ_C 168.69, 168.23 (C^6, C^8), 156.89 (C^4), 154.32 (C^9), 110.91 (C^5), 108.00 (C^7),

65.04 (C^3), 57.78 (C^1), 56.61 (C^{10}), 54.55 (C^2); HRMS$^+$: m/z = 711.1459 $[M+H]^+$ ($C_{30}H_{34}N_6O_9Y$ requires 711.1446).

[Eu.L^4]

Prepared using de-protected ligand (12.4 mg, 19 µmol, 1 eq), $EuCl_3.6H_2O$ (8.1 mg, 22 µmol, 1.2 eq). Purification by reverse phase HPLC (ACE C18-PFP, method C) to afford [**Eu.L^1**] (7.9 mg, 10 µmol, 55%) as a white powder; HRMS$^+$: m/z = 773.1580 $[M+H]^+$ ($C_{30}H_{34}N_6O_9Eu$ requires 773.1560); λ_{abs} = 268 nm; τ_{H2O} = 0.90 ± 0.01 ms; τ_{D2O} = 1.39 ± 0.01 ms.

[Yb.L^4]

Using deprotected ligand (12.4 mg, 19 µmol, 1 eq), $YbCl_3.6H_2O$ (8.6 mg, 22 µmol, 1.2 eq). Purification by reverse phase HPLC (ACE C18-PFP, method C) proceeded as described to afford [**Eu.L^4**] (8.2 mg, 10 µmol, 56%) as a white powder; HRMS$^+$: m/z = 792.1751 $[M+H]^+$ ($C_{30}H_{34}N_6O_9Yb$ requires 792.1735); λ_{abs} (H_2O) = 267 nm.

Synthesis of [Ln.L^5]

Methyl 6-(((methylsulfonyl)oxy)methyl)-4-chloropicolinate

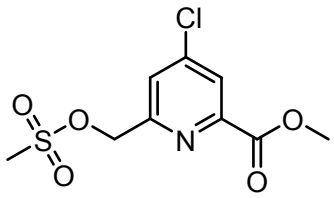

Methyl 4-chloro-6-(hydroxymethyl)picolinate (100 mg, 0.5 mmol, purchased from Fluorochem) was placed under argon and dissolved in anhydrous THF (3 ml). Triethylamine (208 µL, 1.5 mmol) was added followed by dropwise addition of a solution of mesyl anhydride (130 mg, 0.75 mmol) in anhydrous THF (2ml). The reaction was allowed to stir at rt for 1 hr. The solvent was removed under reduced pressure and the residue was dissolved in H_2O (4 mL) and extracted with CH_2Cl_2 (3 x 10 mL). The organic layers were combined and dried over $MgSO_4$ and the solvent removed under reduced pressure. The resulting yellow oil was used immediately (130 mg, 94 %). ^{1}H NMR (400 MHz, $CDCl_3$) δ 8.02 (1H, d, ^4J 1.8, H^3), 7.63 (1H, d, ^4J 1.8, H^5), 5.33 (2H, s, CH_2), 3.94 (3H, s, $COOCH_3$), 3.13 (3H, s, CH_3). ESI-LRMS (+) *m/z* 279.7. ESI-HRMS (+): *m/z* calcd for $C_9H_{11}NO_5SCl$ 280.0046, found 280.0050.

Trimethyl-6,6',6''-(1,4,7-triazacyclononane-1,4,7-triyl)tris(methylene))tris(4-chloropicolinate)

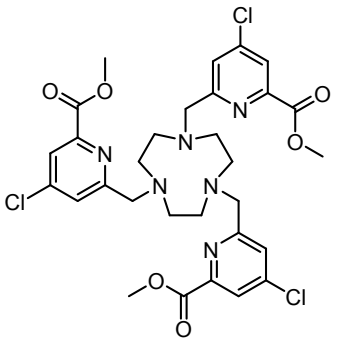

Methyl 6-(((methylsulfonyl)oxy)methyl)-4-chloropicolinate (130 mg, 0.47 mmol), $CsCO_3$ (303 mg, 1.4 mmol) and 1,4,7-triazacyclononane trihydrochloride (37 mg, 0.16 mmol) were dissolved in anhydrous MeCN and stirred at 60 °C under argon for 18 hr. The solution was cooled to rt and filtered to remove inorganic salts. The solvent was removed under reduced pressure and the resulting orange oil was used without further purification. ^{1}H NMR (600 MHz, $CDCl_3$) δ 7.94 (3H, d, ^4J 1.8, H^3), 7.76 (3H, d, ^4J 1.8, H^5), 3.94 (9H, s, CO_2CH_3), 3.93 (6H, s, NCH_2py), 2.88 (12H, s, 9N3 CH_2). ^{13}C NMR (151 MHz, $CDCl_3$) δ 164.7 (CO), 162.7 (C^6), 148.5 (C^4), 145.6 (C^2), 126.2 (C^5), 124.1 (C^3), 64.0 (NCH_2py), 55.9 (9N3 CH_2), 53.1 ($CO_2\underline{C}H_3$).ESI-LRMS (+) *m/z* 679.7. ESI-HRMS (+): *m/z* calcd for $C_{30}H_{34}N_6O_6Cl_3$ 679.1605, found 679.1623.

Yttrium complex of 6,6',6''-((1,4,7- triazacyclononane -1,4,7-triyl)tris(methylene))tris(4-chloropicolinic acid) [Y.L^5]

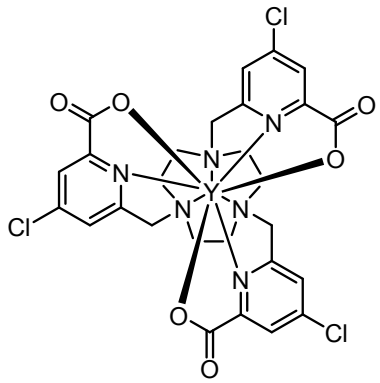

Trimethyl-6,6',6''-(1,4,7-triazacyclononane-1,4,7-triyl)tris(methylene))tris(4-chloropicolinate) (10mg) was dissolved in 0.1 M NaOH (6 ml) and MeOH (6 ml) and stirred at rt for 18 hr. Complete ester cleavage was confirmed by ESI-HRMS (+): *m/z* calcd for $C_{27}H_{28}N_6O_6Cl_3$ 637.1136, found 637.1133. The solvent was removed under reduced pressure to yield a yellow oil which was dissolved in H_2O. The pH of the resulting solution was adjusted to 6 using NaOH and YCl_3 (10 mg, 0.05 mmol) was added. The solution was stirred at rt for 18 h before the solvent was removed under reduced pressure. The resulting yellow solid was purified by reverse-phase HPLC (Waters X-Bridge C18, method E) (t_R = 7.2 min) to yield a white solid. ESI-HRMS (+): *m/z* calcd for $C_{27}H_{25}N_6O_6Cl_3Y$ 722.9960, found 722.9954. ^{1}H NMR (600 MHz, D_2O) δ 7.97 (3H, s, H^3), 7.71 (3H, s, H^5), 3.96 (6H, q,

^2J 14.9, NCH_2py), 3.46 (3H, td, ^2J 14.9, ^3J 4.7, H^{ax}), 2.77 (3H, dd, ^2J 16.4, ^3J 5.7, H^{eq}), 2.52 (3H, dd, ^2J 13.3, ^3J 4.6, $H^{eq'}$), 2.23 (3H, td, ^2J 13.6, ^3J 5.7, $H^{ax'}$).

[Eu.L^5]

An analogous procedure to that described for the synthesis of [Y.L^5] was used (with the lanthanide salt being $EuCl_3 \cdot 6H_2O$), up until the purification stage. The crude solid was dissolved in a 50:50 mix of H2O:MeOH and left to crystallise. After 3 days, X-ray quality crystals were grown and these were used for further measurements. ESI-HRMS (+): *m/z* calcd for $C_{27}H_{25}N_6O_6Cl_3Eu$ 785.0100, found 785.0074.

[Yb.L^5]

An analogous procedure to that described for the synthesis of [Y.L^5] was used (with the lanthanide salt being $YbCl_3 \cdot 6H_2O$). ESI-HRMS (+): *m/z* calcd for $C_{27}H_{25}N_6O_6Cl_3Yb$ 804.0249, found 804.0251.

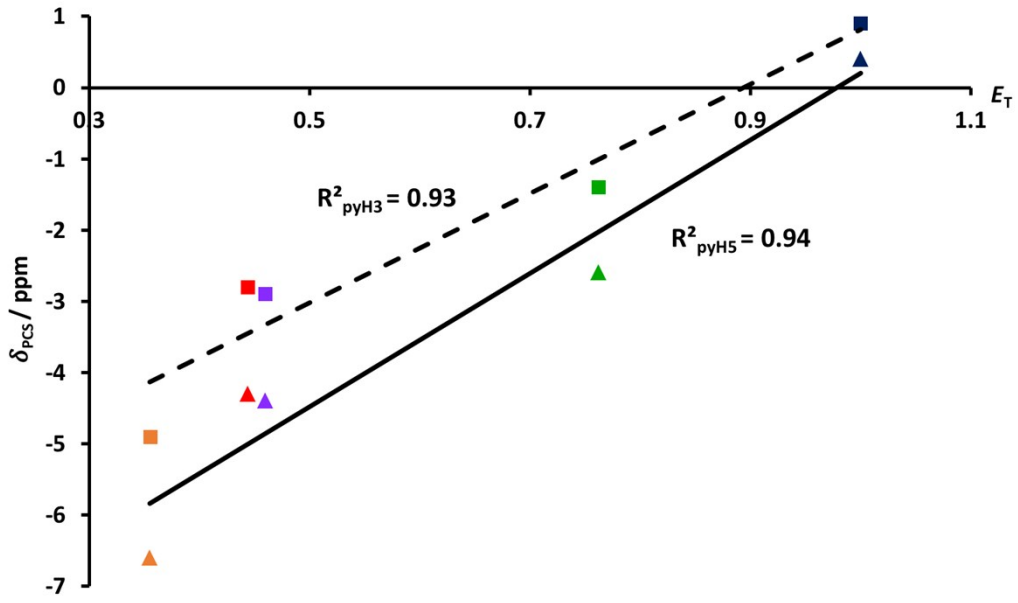

Figure S10 Variation of the paramagnetic chemical shift of selected ligand resonances for [Yb.L^2] with Reichardt's solvent polarity parameter (295 K, 4.7 T). Solvents are labelled as follows: D_2O (*blue*), MeOD (*green*), MeCN-d^3 (*purple*), DMSO-d^6 (*red*) and acetone-d^6 (*orange*).

^{1}H NMR comparison of [Yb.L^2] and[Yb.L^3]

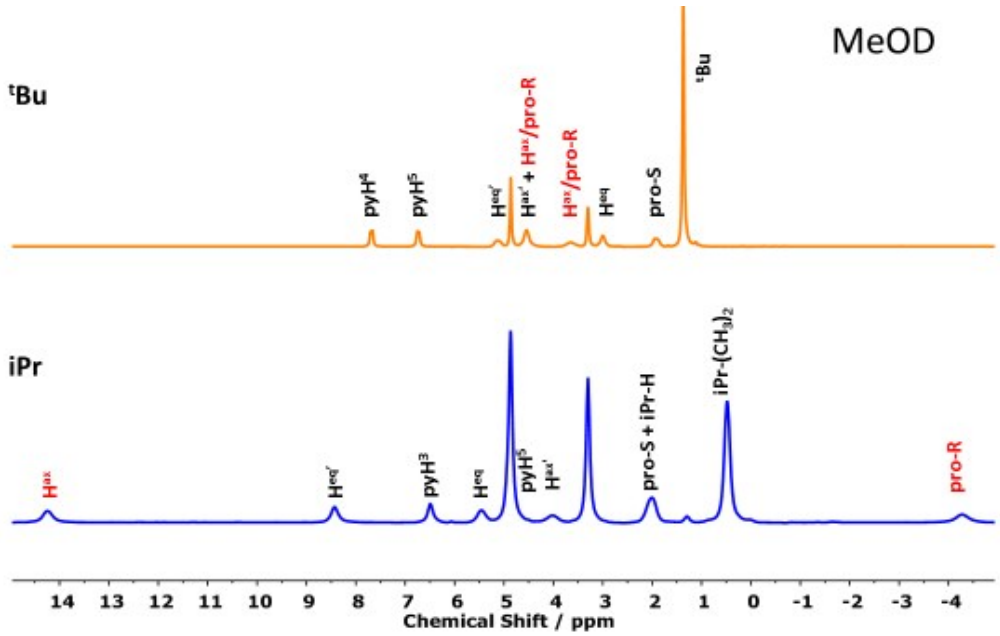

Figure S11 [Yb.L^2] (bottom) and [Yb.L^3] (top) ^{1}H NMR spectra (200 MHz, 295 K). Highlighted in red are H_{ax} and the pro-R hydrogen atom, the two resonances which are most positively and negatively shifted in all [Yb.L^n]

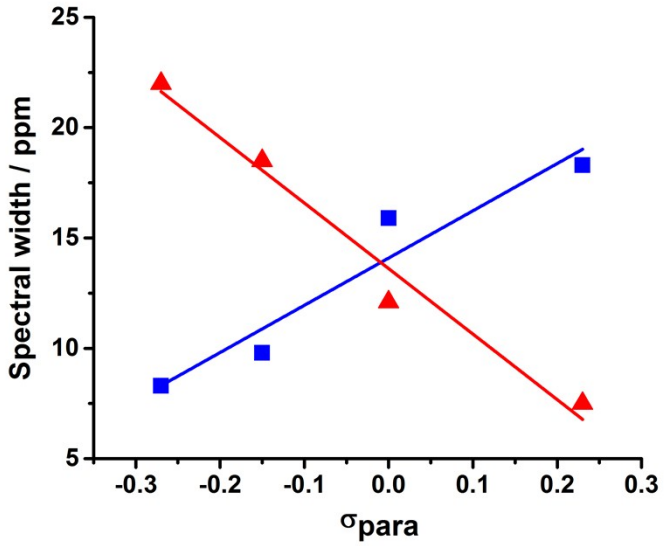

Figure S12 Plot of ^{1}H NMR spectral width against Hammett substituent constant σ_{para} for for Yb complexes of L^1, L^2, L^4 and L^5 in D_2O (blue squares and line) and CD_3OD (red triangles and line), R^2 = 0.93 and 0.97 respectively.

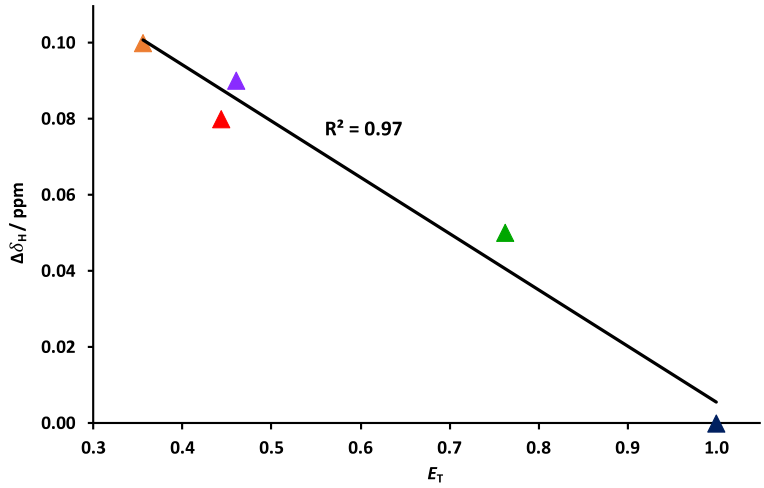

Figure S13 Variation of the chemical shift non-equivalence of the isopropyl Me group resonances with Reichardt's solvent polarity parameter (295 K, 4.7 T) in [Yb.L^2]. Solvents are labelled as follows: D_2O (blue), MeOD (green), MeCN-d^3 (purple), DMSO-d^6 (red) and acetone-d^6 (orange).

Computational methods

Geometry optimisation of the [Yb.L^2] complex was performed with DFT using the software GAUSSIAN 09.[1] Optimisation was performed in presence of SMD solvent model for H_2O using the BP86 functional. The scalar relativistic effects for the Ln atoms are accounted for by using the quadrupole zeta Stuttgart RSC 1997 effective core potential (ECP) basis sets,[2-4] while for C, H, and N atoms the standard GAUSSIAN double zeta Dunning's correlation consistent basis sets (cc-pVDZ) were employed.[5] The optimisation was performed by imposing the C_3 symmetry experimentally observed in NMR using a C_3 symmetric Z-matrix representation of the internal coordinates of atoms in the molecule. CASSCF-SO calculations were performed with the program MOLCAS 8.0[6-8] using the CASSCF/RASSI/SINGLE_ANISO approach.[9-12] For all calculations the Ln atoms were treated with the ANO-RCC-VTZP basis, the N and O donors atoms with the ANO-RCC-VDZP basis, while all other atoms were treated with the ANO-RCC-VDZ basis.[13-16] Relativistic effects were treated in two steps with the second-order DKH Hamiltonian: the scalar relativistic effects were accounted for by using the ANO-RCC basis sets and the spin-orbit coupling was treated explicitly with RASSI. In order to save disk space the two electron integrals were decomposed using the Cholesky decomposition with a high threshold of 10^{-8}. The electronic configuration of $4f^n$ for each of the trivalent lanthanides was modelled with a

complete active space of n electrons in the 7 4*f* orbitals; every CASSCF calculation was checked to ensure the active space was as desired. For [Yb.L^2] 7 configuration state functions (CSFs) were included in the orbital optimisation of the spin-only wave functions for the spin doublet and 7 states were allowed to be mixed by spin-orbit coupling with RASSI. The input structures of [Yb.L^2] for the theoretical study by CASSC-SO of the theta dependence of the anisotropy of the susceptibility tensor, were obatined from the DFT-optimised structure in H_2O by varying the torsion angle of the pyridyl groups in a ±5º range, as previously described.[17]

References- Computational methods

(1) Frisch, M. J.; Trucks, G. W.; Schlegel, H. B.; Scuseria, G. E.; Robb, M. A.; Cheeseman, J. R.; Scalmani, G.; Barone, V.; Petersson, G. A.; Nakatsuji, H.; Li, X.; Caricato, M.; Marenich, A.; Bloino, J.; Janesko, B. G.; Gomperts, R.; Mennucci, B.; Hratchian, H. P.; Ortiz, J. V.; Izmaylov, A. F.; Sonnenberg, J. L.; Williams-Young, D.; Ding, F.; Lipparini, F.; Egidi, F.; Goings, J.; Peng, B.; Petrone, A.; Henderson, T.; Ranasinghe, D.; Zakrzewski, V. G.; Gao, J.; Rega, N.; Zheng, G.; Liang, W.; Hada, M.; Ehara, M.; Toyota, K.; Fukuda, R.; Hasegawa, J.; Ishida, M.; Nakajima, T.; Honda, Y.; Kitao, O.; Nakai, H.; Vreven, T.; Throssell, K.; Montgomery, J. A.; Peralta, J. E.; Ogliaro, F.; Bearpark, M.; Heyd, J. J.; Brothers, E.; Kudin, K. N.; Staroverov, V. N.; Keith, T.; Kobayashi, R.; Normand, J.; Raghavachari, K.; Rendell, A.; Burant, J. C.; Iyengar, S. S.; Tomasi, J.; Cossi, M.; Millam, J. M.; Klene, M.; Adamo, C.; Cammi, R.; Ochterski, J. W.; Martin, R. L.; Morokuma, K.; Farkas, O.; Foresman, J. B.; Fox, D. J. Gaussian 09, Revision A.01. Gaussian, Inc: Wallingford CT 2016.
(2) Dolg, M.; Stoll, H.; Preuss, H.; Pitzer, R. M. J. Phys. Chem. 1993, 97, 5852–5859.
(3) Kaupp, M.; Schleyer, P. v. R.; Stoll, H.; Preuss, H. J. Chem. Phys. 1991, 94, 1360–1366.
(4) Bergner, A.; Dolg, M.; Küchle, W.; Stoll, H.; Preuß, H. Mol. Phys. 1993, 80, 1431–1441.
(5) Dunning, T. H. J. Chem. Phys. 1989, 90, 1007–1023.
(6) Aquilante, F.; De Vico, L.; Ferré, N.; Ghigo, G.; Malmqvist, P.-A.; Neogrády, P.; Pedersen, T. B.; Pitonák, M.; Reiher, M.; Roos, B. O.; Serrano-Andrés, L.; Urban, M.; Veryazov, V.; Lindh, R. J. Comput. Chem. 2010, 31, 224–247.
(7) Veryazov, V.; Widmark, P.-O.; Serrano-Andres, L.; Lindh, R.; Roos, B. O. Int. J. Quantum Chem. 2004, 100, 626–635.
(8) Karlström, G.; Lindh, R.; Malmqvist, P.-Å.; Roos, B. O.; Ryde, U.; Veryazov, V.; Widmark, P.-O.; Cossi, M.; Schimmelpfennig, B.; Neogrady, P.; Seijo, L. Comput. Mater. Sci. 2003, 28, 222–239.
(9) Roos, B. O.; Taylor, P. R.; Siegbahn, P. E. M.; Sigbahn, P. E. M. Chem. Phys. 1980, 48, 157–173.
(10) Roos, B. O. B. O.; Malmqvist, P.-Å. P.-A. Relativistic Quantum Chemistry: The Multiconfigurational Approach; 2004; Vol. 6, p 2919.
(11) Chibotaru, L. F.; Ungur, L. J. Chem. Phys. 2012, 137, 64112.
(12) Ungur, L.; Chibotaru, L. F. Computational Modelling of the Magnetic Properties of Lanthanide Compounds. In Lanthanides and Actinides in Molecular Magnetism; Wiley-VCH Verlag GmbH & Co. KGaA: Weinheim, Germany, 2015; pp 153–184.
(13) Roos, B. O.; Lindh, R.; Malmqvist, P.-Å.; Veryazov, V.; Widmark, P.-O. Chem. Phys. Lett. 2005, 409, 295–299.
(14) Roos, B. O.; Lindh, R.; Malmqvist, P.-Å.; Veryazov, V.; Widmark, P.-O. J. Phys. Chem. A 2005, 109, 6575–6579.
(15) Roos, B. O.; Lindh, R.; Malmqvist, P.-Å.; Veryazov, V.; Widmark, P.-O. J. Phys. Chem. A 2004, 108, 2851–2858.
(16) Veryazov, V.; Widmark, P.-O.; Roos, B. O. Theor. Chem. Accounts Theory, Comput. Model. (Theoretica Chim. Acta) 2004, 111, 345–351.
(17) Vonci, M.; Mason, K.; Suturina, E. A.; Frawley, A. T.; Worswick, S. G.; Kuprov, I.; Parker, D.; McInnes, E. J. L.; Chilton, N. F. J. Am. Chem. Soc. 2017, 139 (40), 14166–14172

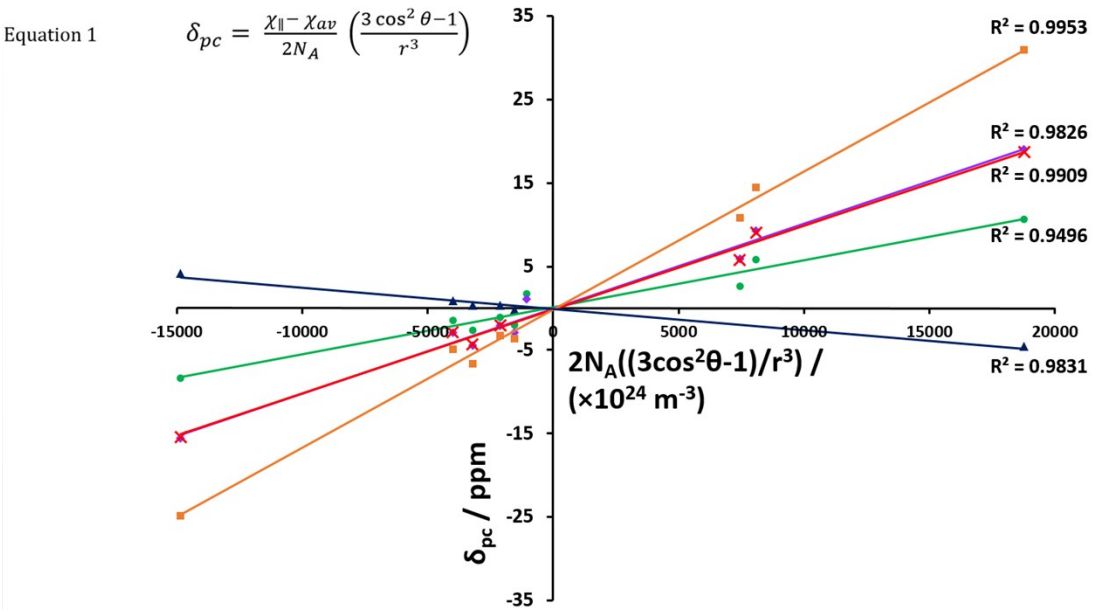

Figure S14 Plot of the experimental δ_{pc} of protons as a function of the structural part of equation 1 for [Yb.L^2] in varying solvents. The magnetic susceptibility anisotropy ($\chi_{\parallel}$-χ_{av}) was extracted as the gradient. Solvents are labelled as follows: D_2O (blue), MeOD (green), MeCN-d^3 (purple), DMSO-d^6 (red) and acetone-d^6 (orange).

Solvent effects in the emission of [Eu.L$^{1\text{-}5}$]

Complementary emission studies of [**Eu.L^2**] in varying solvents focused on the diagnostic $^{\Delta}J = 1$ band. Owing to C_3 symmetry of the [**Ln.L^2**] complexes, the splitting of the $^7F_1$ level was used to independently confirm the effect of solvent polarity on the electronic structure of the Ln(III) complex. In this case, the sign of B_0^2 is negative in all solvents. In polar solvents, the separation between the singlet and doublet energy levels decreases as the solvent varies from DMSO to MeCN to MeOH to H_2O and this corresponds to a decrease in θ. Since the PCS is directly proportional to the crystal field parameter, the overall crystal field splitting and observed NMR shift range should be comparable. Similar values of B_0^2 in DMSO and MeCN are consistent with the lack of difference in the observed NMR spectral width of the Yb(III) analogue in these solvents. The Reichardt's solvent polarity parameter varies very little between DMSO and MeCN (E_T = 0.444 and 0.460 respectively). Hence, it was hypothesised that the solvents induce similar changes in the magnetic susceptibility anisotropy of the Ln(III) complex.

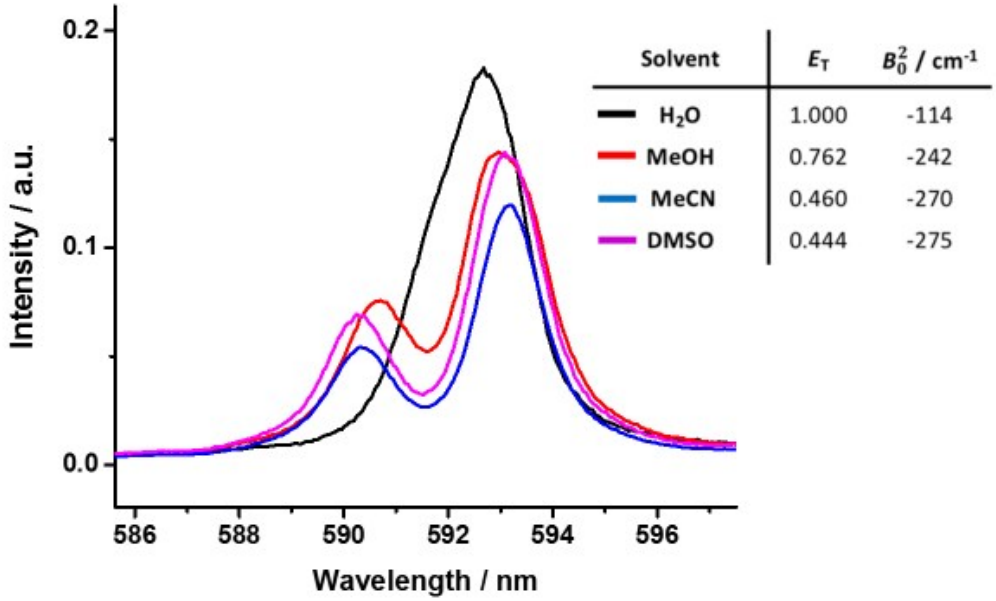

Figure S15 The normalised emission spectra of [Eu.L^2] showing the $^{\Delta}J$ = 1 manifold in the different solvents (295 K, λ_{exc} = 276 nm). Table shows the calculated values of B_0^2 in each solvent.

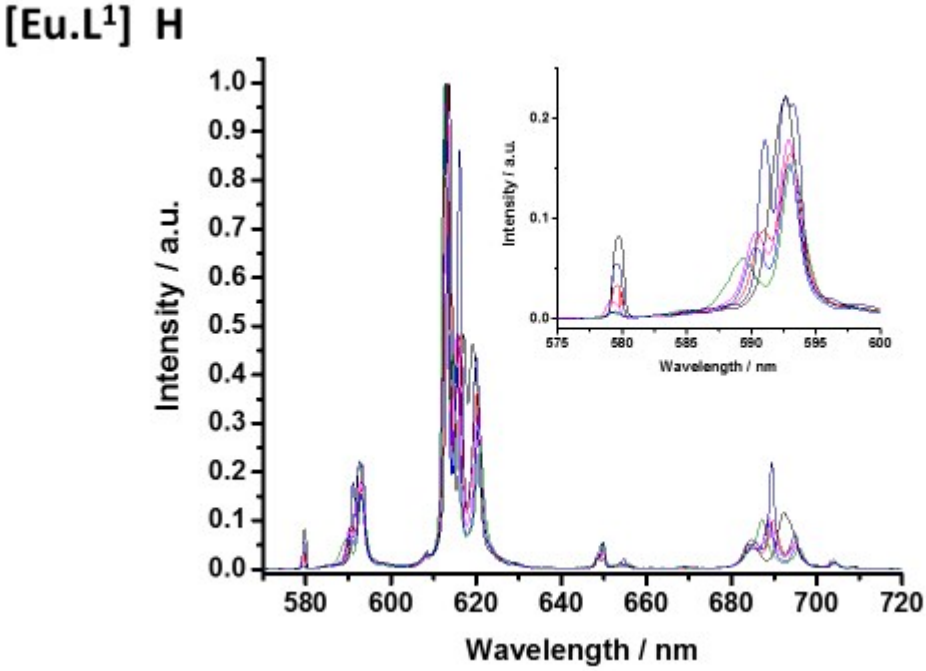

[Eu.L^2] iPr

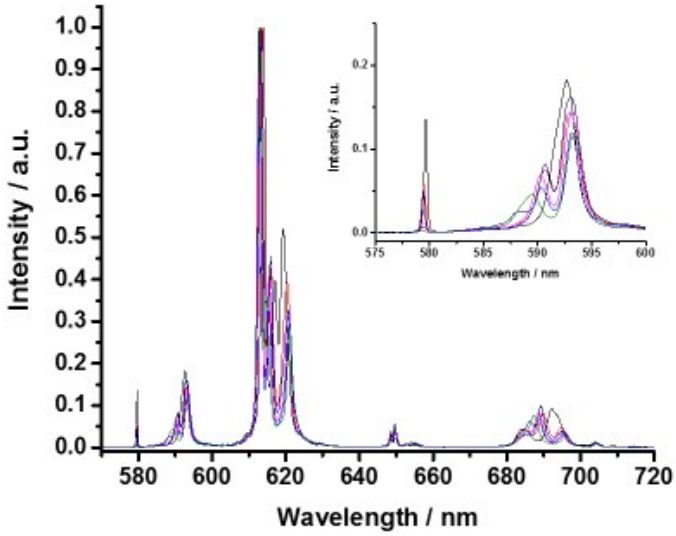

[Eu.L^3] tBu

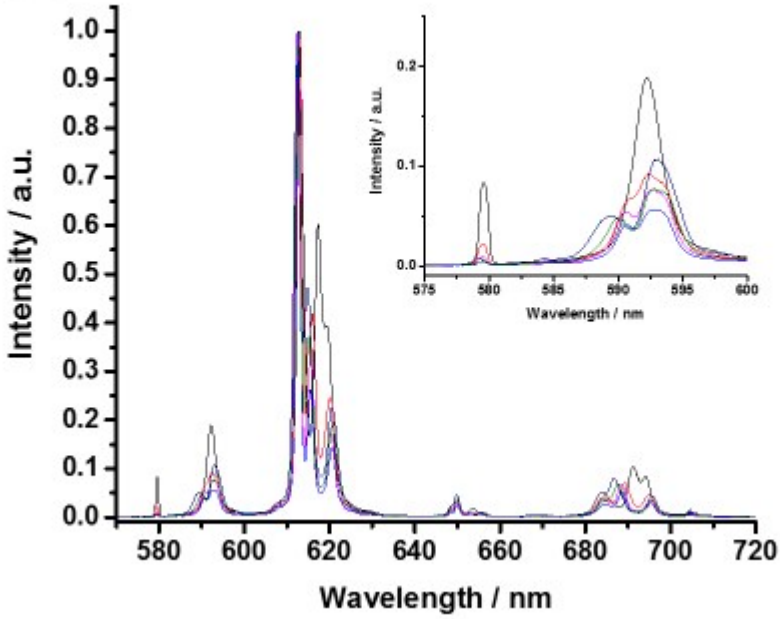

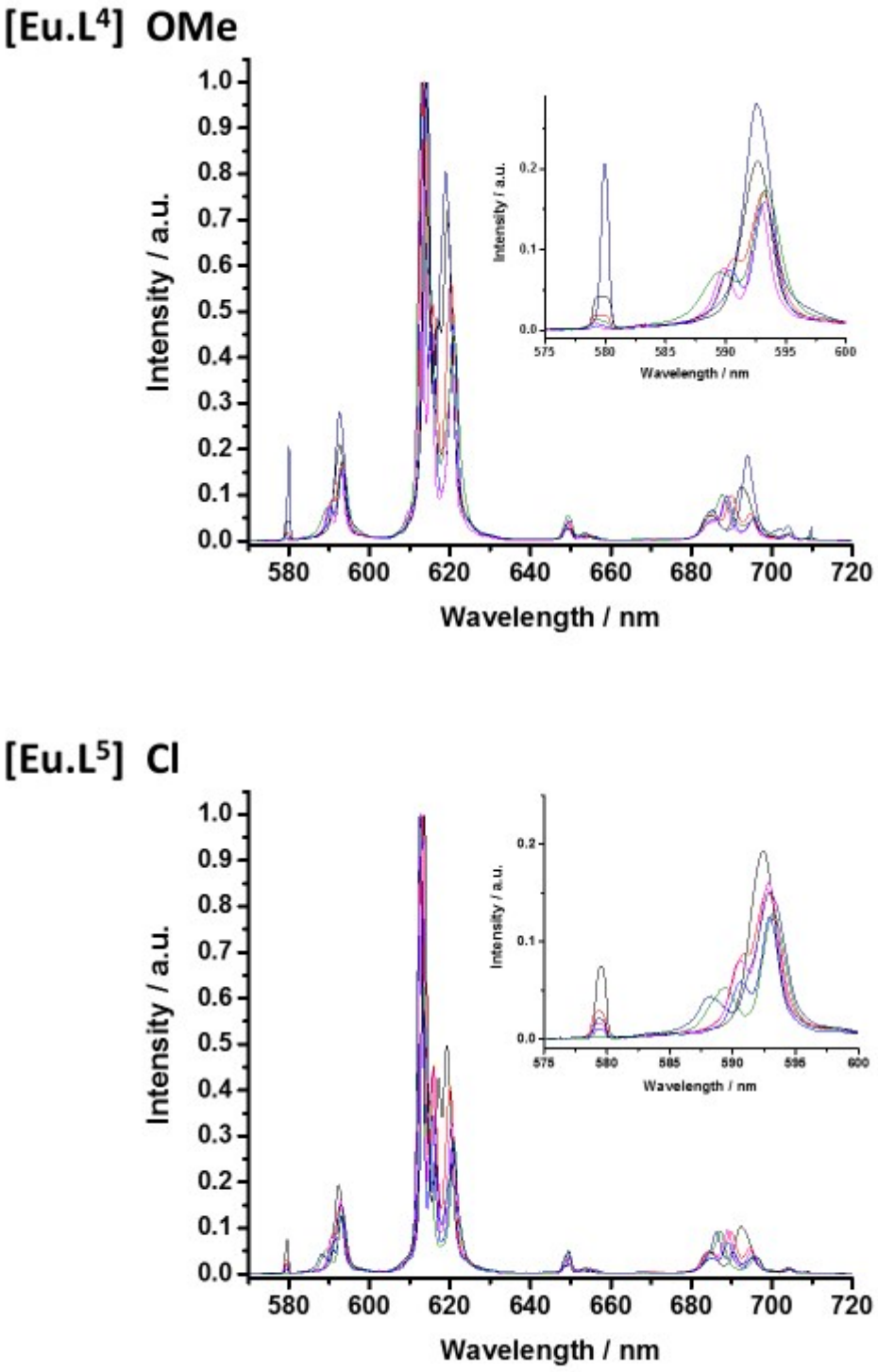

Figure S16 Normalised emission spectra of [Eu.L$^{1\text{-}5}$] in H_2O (black), MeOH (red), MeCN (blue), DMSO (magenta), DCM (green) and chloroform (navy blue). The ΔJ = 1 manifold is expanded in the inset. (298 K, λ_{exc} = 272(L^1), 276(L^2), 286(L^3), 268(L^4), 280(L^5)) .

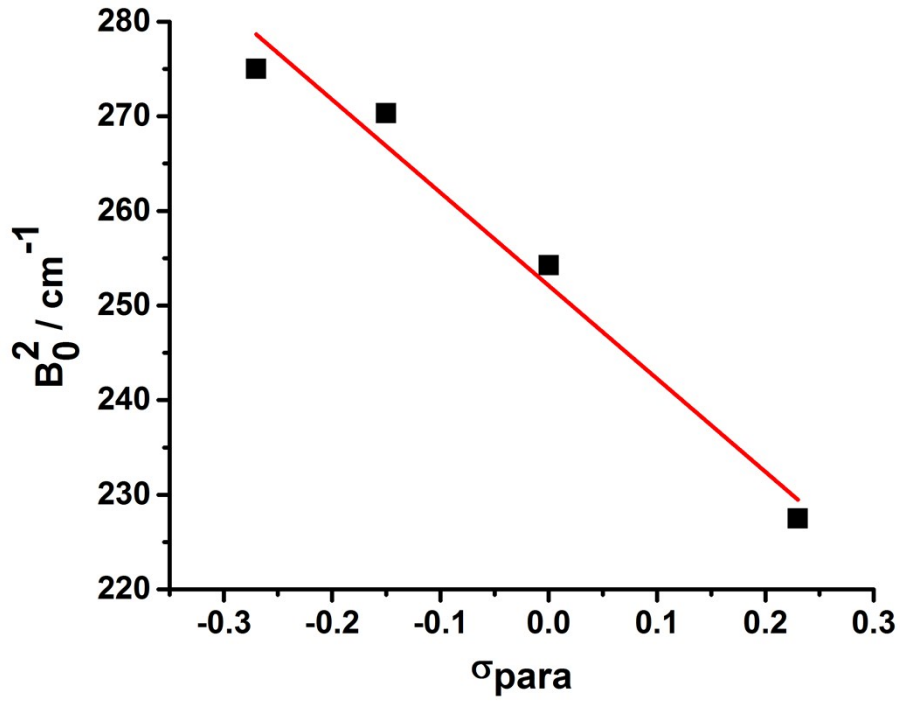

Figure S17 Variation of B_0^2 with the Hammett substituent constant σ_{para}, $R^2 = 0.97$, for Eu complexes of L^1,L^2,L^4 and L^5 in MeCN.

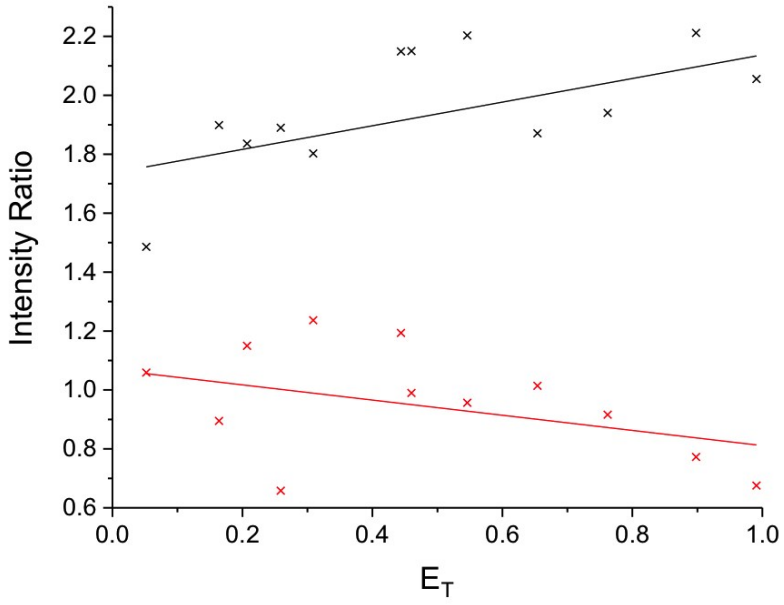

Figure S18 Ratios of the intensity of successive pairs of emission bands (*black*) and B vs. C (*red*) in the $\Delta J = 2$ manifold , as a function of solvent polarity for [Eu.L^4].

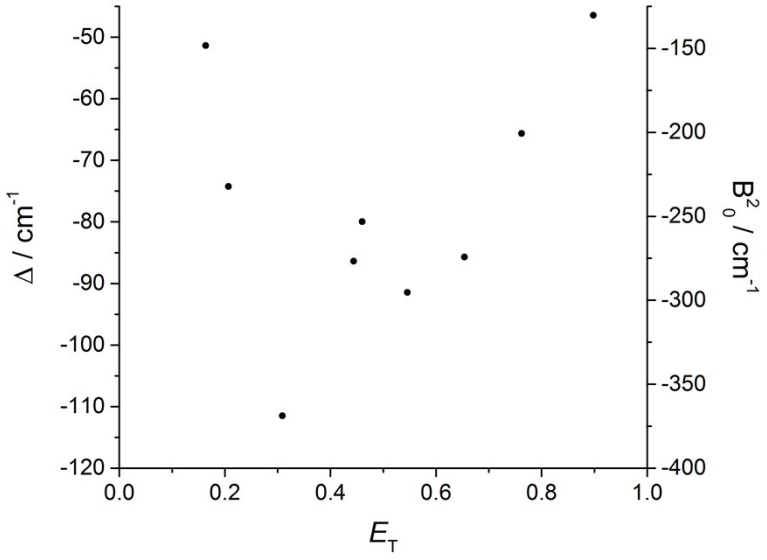

Figure S19 Correlation between Reichardt's solvent polarity parameter (see Table S3, below) and the ligand field coefficient B_0^2, for the complex [Eu.L^4]. The absence of a significant correlation in aprotic media is particularly apparent.

Table S3 Solvent polarity parameters and viscosities for the range of solvents used throughout this work.

Solvent	**Reichardt Solvent Polarity Parameter E_T**	**Absolute Viscosity at 25 °C / cP**
Water	1.000	0.89
2,2,2-Trifluoroethanol (TFE)	0.898	1.7
Methanol	0.762	0.60
Ethanol	0.654	1.08
Propan-2-ol	0.546	2.0
Acetonitrile	0.460	0.38
Dimethylsulfoxide (DMSO)	0.444	2.0
Dichloromethane	0.309	0.44
Chloroform	0.259	0.57
Tetrahydrofuran (THF)	0.207	0.55
1,4-Dioxane	0.164	1.3
Tetrachloromethane	0.052	0.97